Article

Current Biology

Identification of the sex-determining factor in the liverwort *Marchantia polymorpha* reveals unique evolution of sex chromosomes in a haploid system

Graphical abstract

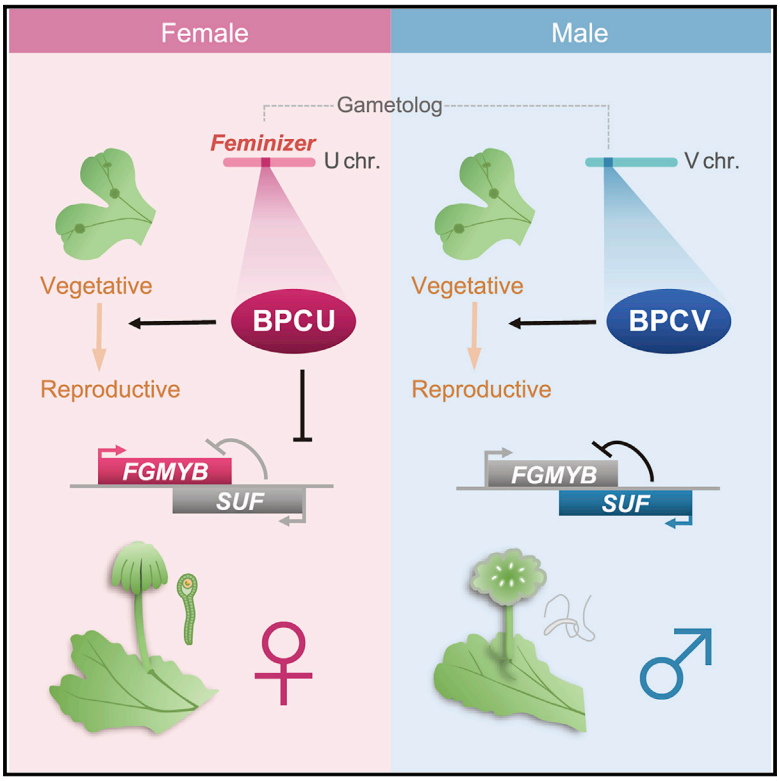

Highlights

- *Feminizer* (*BPCU*) linked to the liverwort female sex chromosome was identified
- *BPCU* regulates the autosomal sex-determining locus, *FGMYB/SUF*
- *BPCU* additionally shares a function for reproductive induction with its gametolog
- The liverwort sex chromosomes are the oldest among any other known systems

Authors

Miyuki Iwasaki, Tomoaki Kajiwara, Yukiko Yasui, ..., Katsuyuki T. Yamato, John L. Bowman, Takayuki Kohchi

Correspondence

john.bowman@monash.edu (J.L.B.), tkohchi@lif.kyoto-u.ac.jp (T.K.)

In brief

Iwasaki et al. identify a female sex determinant, *Feminizer*, on the female sex chromosome of a haploid plant, *Marchantia polymorpha.* Unexpectedly, *Feminizer* also plays a role in reproductive induction, which is shared by its male gametolog. The liverwort sex chromosomes diverged around 430 mya, older than any known sex chromosome systems.

Iwasaki et al., 2021, Current Biology *31*, 5522–5532
December 20, 2021
https://doi.org/10.1016/j.cub.2021.10.023

CellPress

CellPress
OPEN ACCESS

Current Biology

Article

Identification of the sex-determining factor in the liverwort *Marchantia polymorpha* reveals unique evolution of sex chromosomes in a haploid system

Miyuki Iwasaki,[1] Tomoaki Kajiwara,[1] Yukiko Yasui,[1] Yoshihiro Yoshitake,[1] Motoki Miyazaki,[1] Shogo Kawamura,[1] Noriyuki Suetsugu,[1] Ryuichi Nishihama,[1,2] Shohei Yamaoka,[1] Dierk Wanke,[3] Kenji Hashimoto,[2] Kazuyuki Kuchitsu,[2] Sean A. Montgomery,[4] Shilpi Singh,[5] Yasuhiro Tanizawa,[6] Masaru Yagura,[6] Takako Mochizuki,[6] Mika Sakamoto,[6] Yasukazu Nakamura,[6] Chang Liu,[7] Frédéric Berger,[4] Katsuyuki T. Yamato,[8] John L. Bowman,[5,*] and Takayuki Kohchi[1,9,*]
[1]Graduate School of Biostudies, Kyoto University, Kyoto 606-8502, Japan
[2]Faculty of Science and Technology, Tokyo University of Science, Noda, Chiba 278-8510, Japan
[3]Department Biologie I, Ludwig-Maximilians-University (LMU), München 80638, Germany
[4]Gregor Mendel Institute (GMI), Austrian Academy of Sciences, Vienna Biocenter (VBC), 1030 Vienna, Austria
[5]School of Biological Sciences, Monash University, Melbourne, VIC 3800, Australia
[6]National Institute of Genetics, Research Organization of Information and Systems, Mishima, Shizuoka 411-8540, Japan
[7]Institute of Biology, University of Hohenheim, Stuttgart 70599, Germany
[8]Faculty of Biology-Oriented Science and Technology (BOST), Kindai University, Kinokawa, Wakayama 649-6493, Japan
[9]Lead contact
*Correspondence: john.bowman@monash.edu (J.L.B.), tkohchi@lif.kyoto-u.ac.jp (T.K.)
https://doi.org/10.1016/j.cub.2021.10.023

SUMMARY

Sex determination is a central process for sexual reproduction and is often regulated by a sex determinant encoded on a sex chromosome. Rules that govern the evolution of sex chromosomes via specialization and degeneration following the evolution of a sex determinant have been well studied in diploid organisms. However, distinct predictions apply to sex chromosomes in organisms where sex is determined in the haploid phase of the life cycle: both sex chromosomes, female U and male V, are expected to maintain their gene functions, even though both are non-recombining. This is in contrast to the X-Y (or Z-W) asymmetry and Y (W) chromosome degeneration in XY (ZW) systems of diploids. Here, we provide evidence that sex chromosomes diverged early during the evolution of haploid liverworts and identify the sex determinant on the *Marchantia polymorpha* U chromosome. This gene, *Feminizer*, encodes a member of the plant-specific BASIC PENTACYSTEINE transcription factor family. It triggers female differentiation via regulation of the autosomal sex-determining locus of *FEMALE GAMETOPHYTE MYB* and *SUPPRESSOR OF FEMINIZATION*. Phylogenetic analyses of *Feminizer* and other sex chromosome genes indicate dimorphic sex chromosomes had already been established 430 mya in the ancestral liverwort. *Feminizer* also plays a role in reproductive induction that is shared with its gametolog on the V chromosome, suggesting an ancestral function, distinct from sex determination, was retained by the gametologs. This implies ancestral functions can be preserved after the acquisition of a sex determination mechanism during the evolution of a dominant haploid sex chromosome system.

INTRODUCTION

Sex-specific gene expression leading to sexual differentiation is generally triggered by a sex-determining gene, often carried by a sex chromosome. Since the early 20th century, different sex determination systems by sex chromosomes, including XX/XY, ZW/ZZ, XX/XO, and ZO/ZZ, have been described in animals.[1] Similarly, some flowering plants possess XX/XY (or ZW/ZZ) systems directing sex-specific differentiation, leading to flower development during the diploid life phase.[2–4] Sex chromosomes in some flowering plants, including persimmon[2] and poplar,[5] have a single master gene that directs sex determination, as in some animal XX/XY systems. In other flowering plants, such as kiwifruit[6] and asparagus,[7] however, sex determination involves allelic differences in two linked genes on the heterogametic sex chromosome, which act to promote male development and suppress female development.[8] It is also notable that sex chromosomes in a number of dioecious angiosperm species are homomorphic or show minor structural divergence.[9] In diploid systems, suppression of recombination between the sex chromosomes in heterozygotes restricts structural and functional differentiation to the sex chromosome specific to either males (Y) or females (W). The other sex chromosome (X or Z) remains similar to the ancestral state, carrying functional copies of ancestrally present genes, whose presence allows genetic degeneration of the Y- or W-linked regions, sometimes including loss of most ancestral genes. Dosage compensation may evolve to compensate for males' low X-linked gene expression in XY

systems (or females' low Z expression in ZW systems). Understanding of sex determination mechanisms and sex chromosome evolution has largely come from studying diploid organisms.

In contrast to animals and flowering plants, sexual differentiation takes place in the dominant haploid life phase of bryophytes (e.g., liverworts and mosses) and most algae,[10,11] with species with separate male and female individuals termed dioicous. In these groups, males and females are defined by their gamete size, with females producing large immotile egg cells and males producing small motile sperm.[12,13] Sex chromosomes in haploid systems show fundamentally distinct genetic and evolutionary behavior from those in diploid systems in which one sex is hemizygous (XY or ZW) and one homozygous (XX or ZZ).[14,15] In haploid systems, each individual carries only a single sex chromosome. The female and male sex chromosomes are termed U and V, respectively, to emphasize the differences from X and Y (or Z and W) chromosomes.[16] Fertilization results in diploid UV sporophytes, a brief non-sexually differentiated phase of the life cycle, another difference from diploid systems. Due to their similar inheritance, the U and V chromosomes are predicted to evolve similarly.[14] Specifically, both chromosomes are predicted to undergo little or no degeneration, and any degeneration is predicted to affect both the U and V chromosomes similarly, in contrast to the diploid systems outlined above.[17]

Many liverwort species are dioicous and often have heteromorphic sex chromosomes,[18] and dioicy is the likely ancestral condition for liverworts. In *Marchantia polymorpha*, plants possess either a U or a V sex chromosome[19–21] and develop into females or males, respectively. Genetic analyses of phylogenetically diverse liverworts indicate that the U chromosome carries a feminizing locus and that the V chromosome carries multiple loci required for sperm motility.[18] Further, haploid plants spontaneously containing both U and V chromosomes develop as females, supporting the presence of a dominant U-linked feminizing locus,[22] in whose absence plants develop as males. Genomic analyses of *M. polymorpha* have shown that both U and V chromosomes have lower gene densities, and higher repetitive content, than the autosomes,[19–21] similar to the symmetrical changes in other non-recombining U/V systems, in the mosses *Ceratodon purpureus*[23] and *Syntrichia caninervis*[24] and the brown alga *Ectocarpus*.[25] However, the sex-determining genes have yet to be identified in liverworts or any other complex multicellular haploid organism, and only recently has it become possible to study the evolution of sex chromosomes in haploid systems and test their predicted differences from diploid systems.

Here, we identify a U-linked transcription factor gene, *BASIC PENTACYSTEINE ON THE U CHROMOSOME* (*BPCU*), as the master sex determinant, *Feminizer*, in *M. polymorpha*. *BPCU* has a homolog (gametolog) on the V chromosome, *BASIC PENTACYSTEINE ON THE V CHROMOSOME* (*BPCV*), and both share a conserved function in reproductive induction, suggesting retention of an ancestral function despite the *BPCU* gametolog evolving an additional function in female sex determination. Phylogenetic analyses of *BPCU* and *BPCV*, and their orthologs in other liverworts suggest that these gametologs, and thus the U and V chromosomes, had been already established 430 mya in the ancestral liverwort.

RESULTS

Chromosome-level assembly of the U chromosome

As a basis for the search for *Feminizer*, we constructed a chromosome-level assembly of the U chromosome using PacBio long-read sequencing and Hi-C[26] technologies, as was done previously for the V chromosome.[20] The U chromosome carries rDNA repeats at each of its ends[21,27] and, between these, includes a 4.5-Mb region containing genes. Previous analyses identified 74 and 154 genes on the U and V chromosomes, respectively,[19,21] but the chromosome-level assembly of the U chromosome and manually refined annotation of both chromosomes (excluding transposable element genes and merging some split genes) result in smaller numbers of 47 and 93, respectively (Data S1A). As was noted previously,[19] most U chromosome genes that do not have a V gametolog appear to be fragmentary or have highly similar autosomal paralogs, suggesting that they may be recent immigrants to the U chromosome (Data S1A). The eight *M. polymorpha* autosomes carry much larger numbers of genes, between 1,900 and 3,000.[20]

BPCU on the U chromosome is necessary and sufficient for female sex determination

We confirmed the aforementioned predictions of a dominant U-linked sex-determining *Feminizer* locus in *M. polymorpha*,[22] because plants carrying both U and V sex chromosomes that arose spontaneously via meiotic non-disjunction (wild type [WT] [UV], the sex chromosome background is given in brackets for clarity) developed female sex organs (Figures 1A–1C). To identify the U-linked *Feminizer* gene, we screened, via genome editing of U-chromosome candidate genes, for mutations that impact sex organ morphology (Data S1A). Two independently obtained mutants of *BPCU* formed male sex organs (Figures 1D–1F), suggesting that *BPCU* is necessary for development of female sex organs. Surprisingly, both of these *bpcU* mutants possessed not only a U chromosome harboring the mutated *bpcU* gene but also a V chromosome (Figure 1G). This observation and analysis by flow cytometry (Figure S1) suggest that the two *bpcU* mutants were derived from spores that had inherited both sex chromosomes, presumably via non-disjunction. To further test BPCU's dominant feminizing activity, we introduced a genomic fragment of *BPCU* spanning 2 kb upstream to 3 kb downstream of the *BPCU* transcribed region into the genome of WT male plants that carry only the V chromosome. The genetically male plants transformed with *BPCU* (g*BPCU* [V]) displayed a male-to-female sex conversion phenotype, although no egg cells developed within their sex organs (Figure 1H), a phenotype previously reported for an autosomal sex conversion mutant.[28] The loss of egg cell differentiation in these genotypes is likely due to the lack of U-linked egg-cell differentiation gene(s). We concluded that *BPCU* is necessary and sufficient to induce the development program of female sex organs.

BPCU acts as *Feminizer* by regulating the autosomal sex-determining locus, *FGMYB/SUF*

We next analyzed the expression profiles of sex-specific genes[28] in the sex-converted plants and detected gene

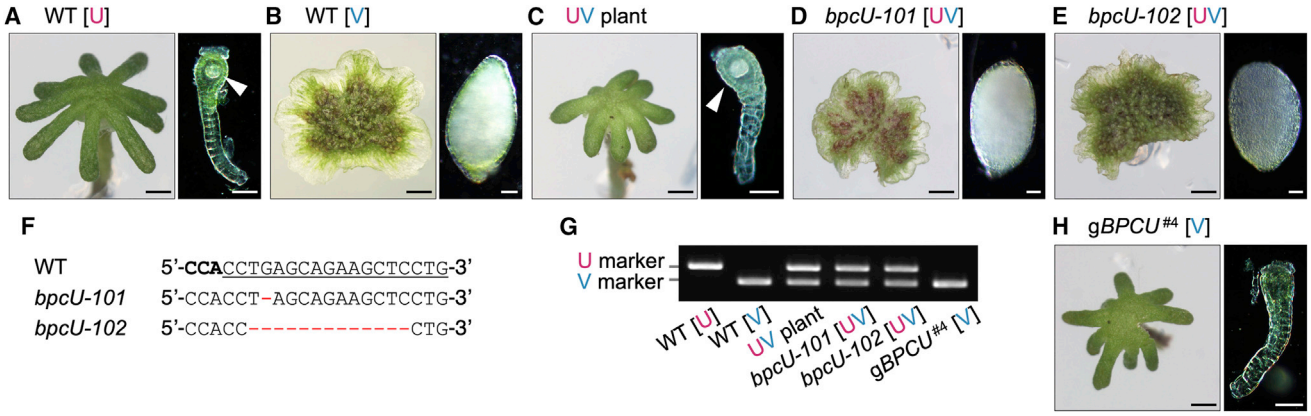

Figure 1. *BPCU* on the U chromosome is necessary and sufficient for female sex determination

(A–E) Sexual development of wild-type (WT) and mutant plants. Sex organs of female and male WT plants are shown in (A) and (B), respectively. Photographs were taken from female WT [U] (Tak-2; A), male WT [V] (Tak-1; B), UV plant (C), genome-editing mutants of *bpcU* (*bpcU-101* [UV], D; *bpcU-102* [UV], E). Left and right panels: receptacles and gamete-containing organs are shown, respectively. Arrowheads indicate egg cells. Scale bars, 1 mm (left panels); 50 μm (right panels).

(F) Mutations in *bpcU*. The nucleotide sequences of the WT and the mutants (*bpcU* [UV]) are aligned. The sequence for guide RNA (gRNA) for genome editing is underlined. The protospacer adjacent motif (PAM) sequence for CRISPR/Cas9 is shown in bold. Deletions are shown in red.

(G) Diagnosis of genetic sex using U-chromosome- and V-chromosome-linked markers.

(H) Feminization of the genetic male lines transformed with *BPCU* (g*BPCU* [V]). Sex organs 1 month after reproductive induction are shown for g*BPCU*$^{\#4}$ [V]. Left and right panels; receptacle and gamete-containing organ are shown, respectively. Scale bars, 1 mm (left panel); 50 μm (right panel).

See also Figure S1.

expression patterns reflecting the morphological sex phenotype (Figure 2A). Critically, expression of the autosomal locus *FEMALE GAMETOPHYTE MYB* (*FGMYB*), which promotes female sex differentiation,[28] was correlated with the morphological sex observed in different genotypes. In males, the expression of *FGMYB* is suppressed by expression of an antisense long non-coding RNA called *SUPPRESSOR OF FEMINIZATION* (*SUF*), which is transcribed from a promoter located 3′ of the *FGMYB* locus.[28] Consistent with the sex conversion phenotype, the mutants (*bpcU-101* and *bpcU-102*) had decreased *FGMYB* and increased *SUF* expression compared with WT females (Figure 2B, left). Furthermore, the *BPCU*-carrying genetically male plants (g*BPCU* [V]) had decreased *SUF* and increased *FGMYB* expression compared with WT males (Figure 2B, right).

BPCU belongs to an alanine-zipper-containing group of the BARLEY B RECOMBINANT/BASIC PENTACYSTEINE (BBR/BPC) proteins that bind to GAGA elements[31,32] and repress gene expression via epigenetic regulation.[32] We demonstrated that, *in vitro*, BPCU binds to GAGA motifs enriched in the promoter of *SUF* (Figure S2). Thus, we hypothesized that, in females, BPCU directly suppresses *SUF* expression, consequently relieving *FGMYB* from suppression by *SUF*. In support of this hypothesis, *fgmyb* mutations in the g*BPCU* [V] background suppressed the feminization induced by g*BPCU* (Figures 2C and S3). We also observed differences in chromatin status with the repressive H3K27me3 peaks expanded into the gene region of *SUF* in WT [U], but not in WT [V] and *bpcU* [U] (Figure 2D), which is consistent with a model that BPCU directly represses *SUF* through chromatin modification. These observations indicate that *BPCU* acts as the U-linked *Feminizer* and that it directly regulates the autosomal sex-determining locus complex, *FGMYB/SUF*, in *M. polymorpha*.

BPCU and its gametolog, *BPCV*, are required for induction of sexual reproduction, but only *BPCU* confers the feminization

In contrast with other sex-determining genes identified in diploid organisms and also in the haploid alga *Volvox carteri*,[33] the *Feminizer*, *BPCU*, has a paired homolog, *BPCV*, on the male sex chromosome (Figure S4A). Such gene pairs are called "gametologs" and originate from a common ancestral autosomal gene. Gametologs generally conserve essential functions that are maintained during sex chromosome evolution. Indeed, the highly conserved C-terminal domain of BPCV, which is known as a DNA-binding domain of BPCs, also bound the same target sequences as BPCU *in vitro* (Figure S2A). *BPCU* and *BPCV* are both expressed primarily in the female and male reproductive organs, respectively, although they are expressed in all tissues examined (Figure S4B).

Because the *bpcU* mutants (*bpcU-101* and *bpcU-102*) obtained by the initial screening were aneuploid with the V chromosomes, we generated *bpcU* as well as *bpcV* mutants in a haploid background (Figures 3A and S5). Both *bpcU* and *bpcV* haploid mutants failed to induce sex organ formation under growth conditions that induce reproductive development in WT (Figures 3B and 3E). The introduction of a genomic fragment of *BPCU* or *BPCV* complemented the reproductive induction phenotype of *bpcU* (Figures 3C–3E). However, *bpcU* mutants complemented with *BPCV* developed male sex organs instead of female sex organs (Figures 3C and 3D). These observations indicate that *BPCU* and *BPCV* share a function required to induce sex organ development.

The sex chromosomes in liverworts were established around 430 mya, which is the oldest among the known sex chromosomes

We first examined the antiquity of the *BPCU* and *BPCV* gametologs within liverworts and noted that both gametologs are

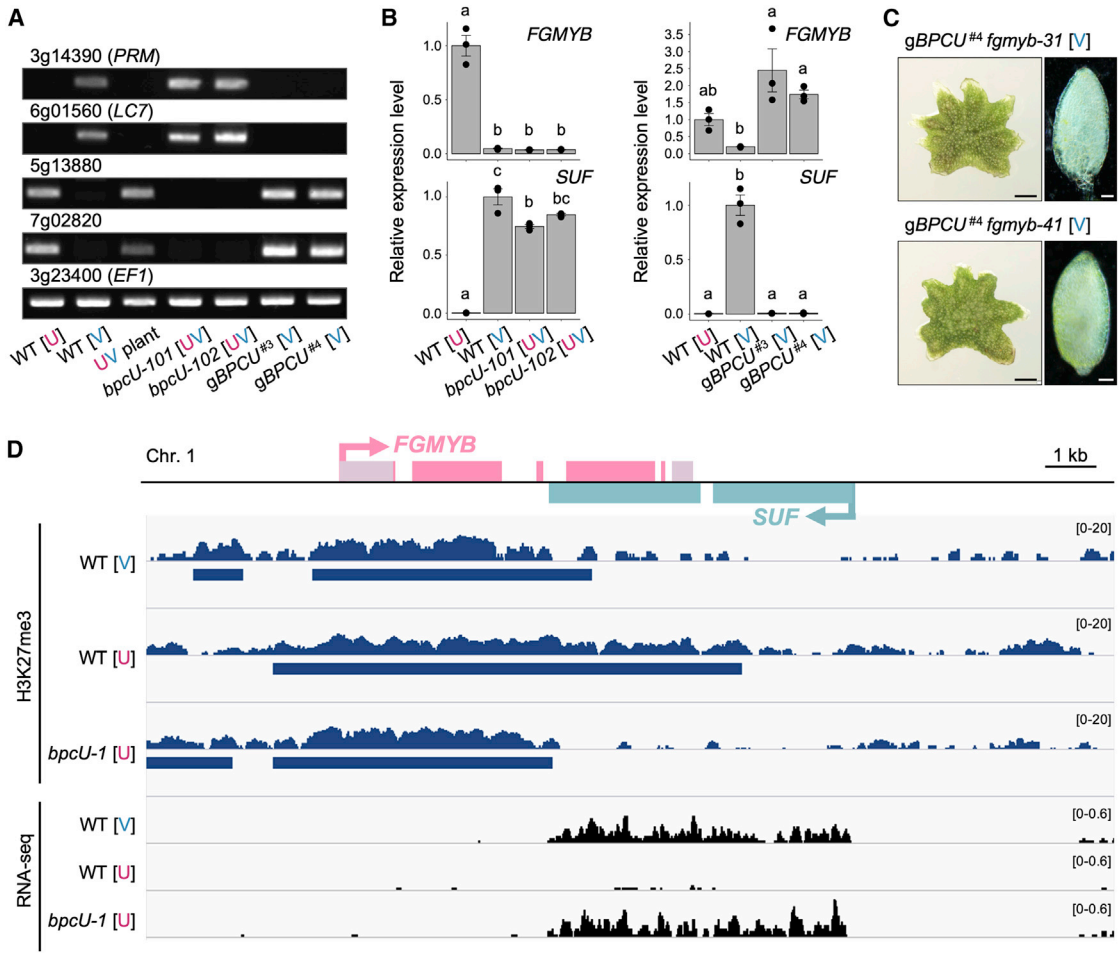

Figure 2. *BPCU* acts as *Feminizer* by regulating the autosomal sex-determining locus, *FGMYB/SUF*

(A) RT-PCR analysis of sex-specific gene expression in *bpcU* [UV] and g*BPCU* [V]. Total RNAs from WT [U] (Tak-2), WT [V] (Tak-1), UV plant, *bpcU* (*bpcU-101* [UV] and *bpcU-102* [UV]), and g*BPCU* [V] (lines no. 3 and no. 4) were used for detecting expression of the genes indicated above. Mp3g14390 and Mp6g01560 are genes expressed specifically in males and Mp5g13880 and Mp7g02820 in females. Mp3g23400 (*EF1*) is a ubiquitously expressed gene.

(B) Expression of *FGMYB* and *SUF*. qRT-PCR was performed for RNAs from sex organs. Experiments shown in the left and right panels were performed separately for the loss-of-function lines (*bpcU-101* [UV]; *bpcU-102* [UV]) and the gain-of-function lines (g*BPCU* [V] no. 3 and no. 4), respectively, with WT [U] (Tak-2) and WT [V] (Tak-1) as controls. Bars represent mean ± SE. Symbols above the bars indicate grouping by $p < 0.05$ in a Tukey-Kramer test ($n = 3$).

(C) Genetic suppression of *BPCU*-dependent feminization by *fgmyb* mutation. Sex organs 1 month after reproductive induction are shown for two independently obtained *fgmyb* mutants. Left and right panels: receptacles and gamete-containing organs are shown, respectively. Scale bars, 1 mm (left panels); 50 μm (right panels).

(D) H3K27me3 status at the *FGMYB/SUF* locus in the vegetative stage in WT [U], WT [V], and *bpcU-1* [U]. See Figure 3 for the genotype and the phenotype of *bpcU-1* [U]. IGV browser screenshot is shown.[29] H3K27me3 and RNA-seq tracks show bigwig files normalized to 1 × genomic coverage (reads per genome coverage [RPGCs]) and bins per million mapped reads (BPMs), respectively (window size = 10 bp). Peak calling was done using SICER2[30] with the default parameters (window size = 200 bp; false discovery rate [FDR] = 0.01). H3 was used as a control for peak calling.

See also Figures S2 and S3.

present in species representing the three extant lineages of liverworts, indicating that the divergence of these gametologs began in the ancestral liverwort (Figure 4). Further, the ancestral land plant possessed a single BPC transcription factor gene,[19,34] a condition likely retained in common ancestors of each of the bryophyte lineages. The identification of *BPCU* as *Feminizer* in *M. polymorpha* sheds light on liverwort U/V sex chromosome evolution. Sex chromosomes have their evolutionary origin when an ancestral gene on an autosomal pair mutates or when a gene duplicates onto one member of this chromosome pair and functions as a sex determiner. During the evolution of a U/V sex chromosome system, the sex-determining gene might have arisen in a non-recombining region or a non-recombining region might have evolved subsequently. Thereafter, successive chromosomal rearrangements could create evolutionary strata of U-V sequence divergence and potential genetic degeneration, which, as outlined above, should affect both members of the pair.[10,14,15] However, essential genes required in the haploid generation could be retained on both the U and V and over time diverge into pairs of gametologs that differ in sequence but retain a conserved function. In contrast, genes necessary in only one sex should be retained

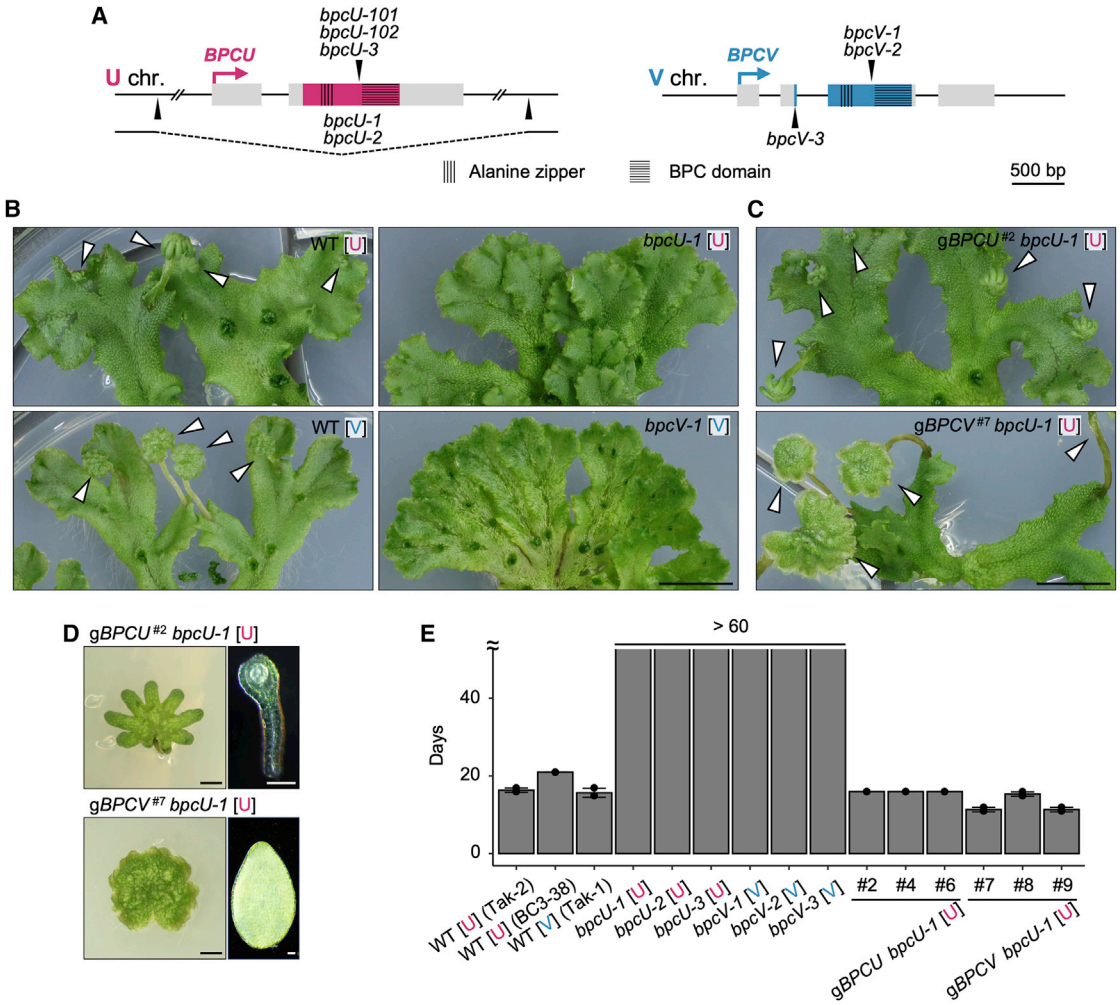

Figure 3. *BPCU* and its gametolog *BPCV* are required for induction of sexual reproduction, but only *BPCU* confers the feminization

(A) Gene organizations of *BPCU* and *BPCV* loci and schematic illustrations of *bpcU* and *bpcV* mutations. The coding regions are colored. Gray boxes indicate 5′ and 3′ untranslated regions. Arrowheads indicate the positions of gRNAs. The deleted region in *BPCU* is shown by a bent broken line.

(B) No sex organ formation in *bpcU* [U] and *bpcV* [V]. Female WT [U] (Tak-2; top left), male WT [V] (Tak-1; bottom left), *bpcU-1* [U] (top right), and *bpcV-1* [V] (bottom right) plants are shown. Images 1 month after reproductive induction are shown. Arrowheads indicate sex organs. Scale bar, 10 mm.

(C) Genetic complementation of the reproductive induction phenotype of *bpcU* with *BPCU* or *BPCV*. Genomic *BPCU*-transformed *bpcU* [U] (g*BPCU*$^{\#2}$ *bpcU-1* [U]; top) and genomic *BPCV*-transformed *bpcU* [U] (g*BPCV*$^{\#7}$ *bpcU-1* [U]; bottom) plants are shown. Arrowheads indicate sex organs. Scale bar, 10 mm.

(D) Magnified images of sex organs in g*BPCU*$^{\#2}$ *bpcU-1* [U] (top) and g*BPCV*$^{\#7}$ *bpcU-1* [U] (bottom). Sex organs 1 month after reproductive induction are shown. Left and right panels: receptacles and gamete-containing organs are shown, respectively. Scale bars, 1 mm (left panels); 50 μm (right panels).

(E) Loss of *BPCU* or *BPCV* impairs reproductive induction. Gemmae were grown under white light for 10 days and transferred to the reproductive induction condition (STAR Methods). Days at which a visible receptacle was first formed after reproductive induction are shown. No sex organs were formed in *bpcU* (*bpcU-1*, *bpcU-2*, and *bpcU-3*) and *bpcV* (*bpcV-1*, *bpcV-2*, and *bpcV-3*) over 60 days. Bars represent mean ± SD (n = 3).

See also Figures S4 and S5.

on the respective sex chromosome and could be lost from the other.[17]

Because the sex-determining gene or genes should be located in the oldest stratum,[10] the *M. polymorpha BPCU* probably identifies the oldest non-recombining region of the U chromosome. In this plant, divergence of U-V genes could not be estimated using synonymous site substitution values (pS), because these values are at or near saturation for almost half of the 19 gametolog pairs (Data S1B). Instead, we therefore used phylogenetic analyses based on all alignable coding sequences of each of the gametologs (Figure 4; Data S2). The timing of the incorporation of each pair of *M. polymorpha* gametologs into non-recombining regions of the *M. polymorpha* sex chromosomes can be inferred by the tree topology. If the *M. polymorpha* U and V gametologs are less diverged from Haplomitriopsida sequences than from each other, the divergence of the *M. polymorpha* gametologs was inferred to have occurred before the divergence of the Haplomitriopsida and the Marchantiopsida. Conversely, if the *M. polymorpha* U and V gametologs are less diverged from one another than they are to some other liverwort sequences, then their divergence time was inferred based on the relative positions in the tree topology of the

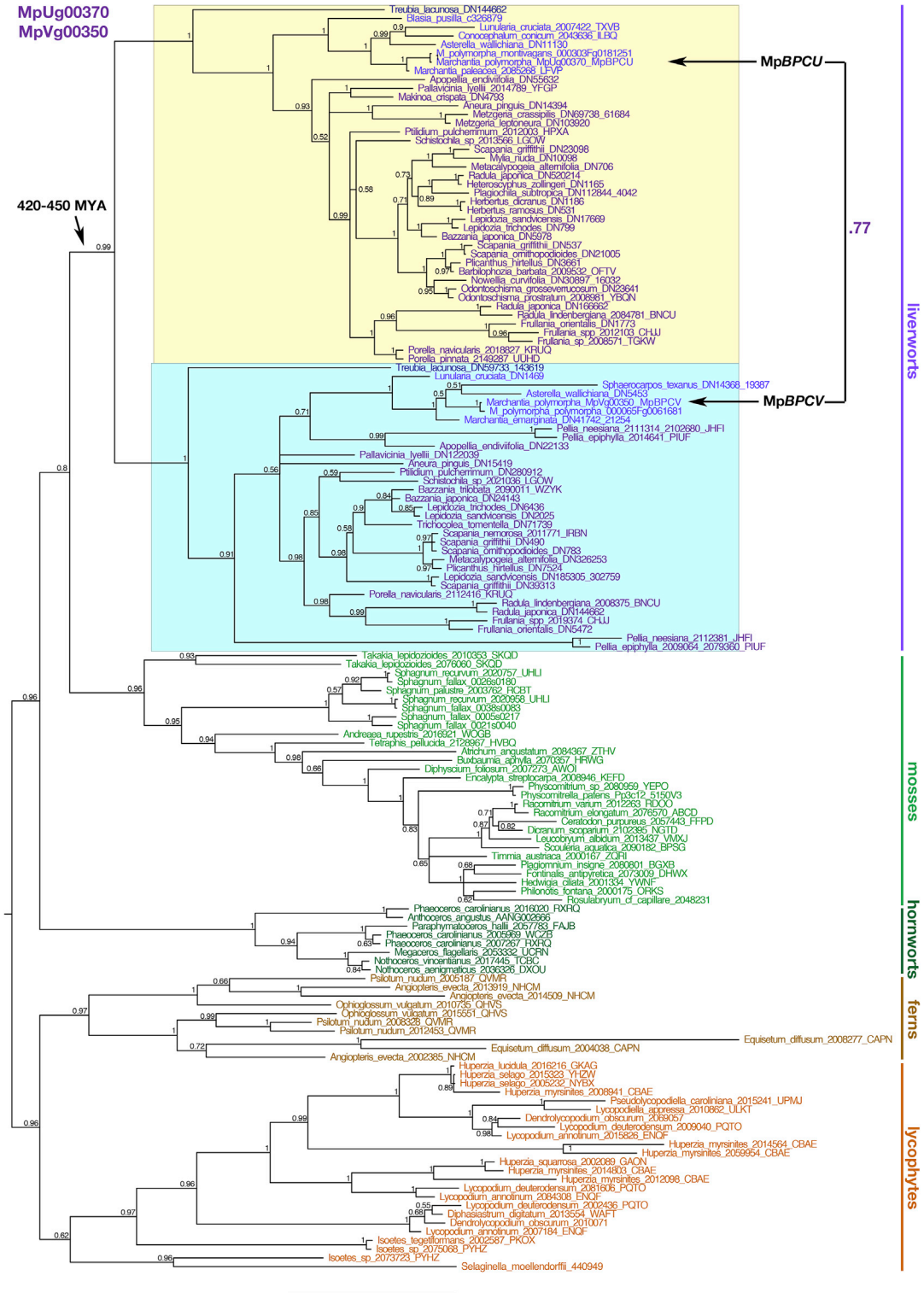

Figure 4. Phylogenetic tree of *BPCU* and *BPCV*

The phylogram was reconstructed using nucleotide alignments as described in the STAR Methods section. The liverwort sequences are shown in purple, and the clades containing *BPCU* and *BPCV* are highlighted in yellow and turquoise, respectively. The phylogenetic positions of the *BPCU* and *BPCV* of *M. polymorpha* are demarcated by arrows with the pS value between the two *M. polymorpha* gametologs indicated (0.77). Taxa are color coded as follows: liverworts, purple; Haplomitriopsida, dark purple; Marchantiopsida, bright purple; Jungermanniopsida, violet; hornworts, dark green; mosses, light green; lycophytes, orange; and ferns, brown. Numbers at branches indicate posterior probability values. See also Data S1B and S2.

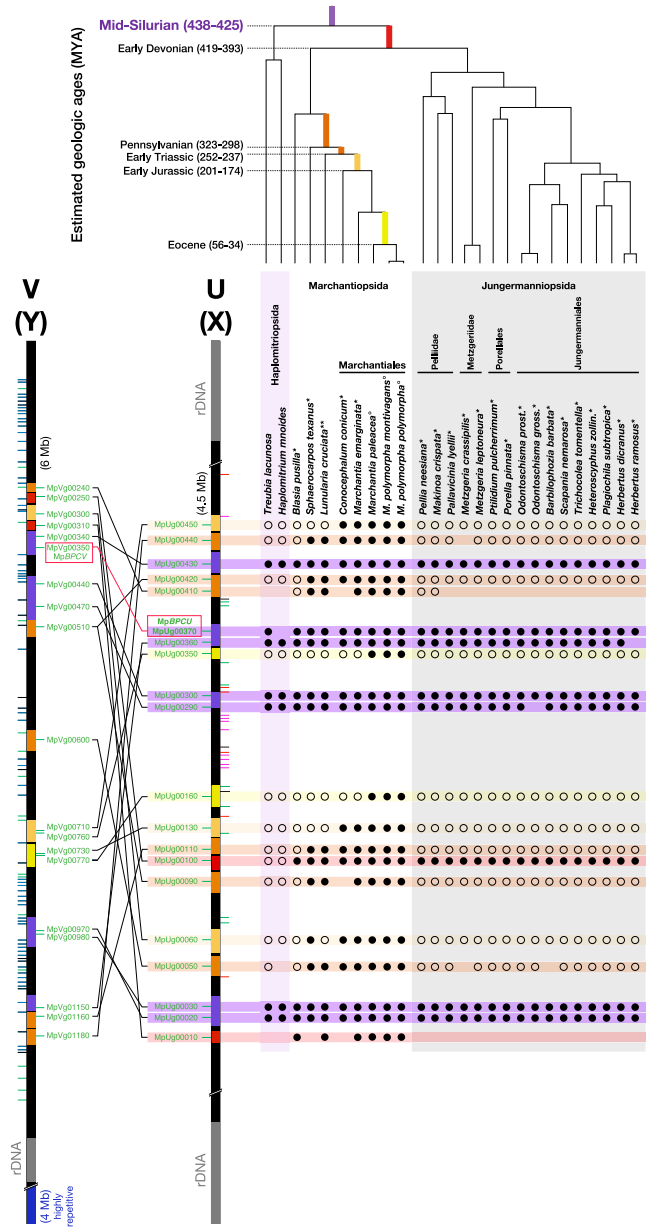

Figure 5. Feminizer and sex chromosome evolution in *M. polymorpha*

A schematic of the genomic architecture of the *M. polymorpha ruderalis* U and V chromosomes is displayed (vertical bars on the left) with gametologs positioned between the chromosomes and U- and V-specific genes represented by short lines (for expression patterns, see Data S1A). The U chromosome sequence was obtained from a chromosome-scale assembly of the female accession, Tak-2; an updated list of its annotated genes is in Data S1A along with V-linked gametologs and previous (v3.1) annotations where applicable. Results of phylogenetic analyses of Marchantiophyta orthologs are presented as a matrix on the right. Open circles indicate outgroup sequences that diverged before the *M. polymorpha* U and V divergence. These were inferred when sequence divergence between the *M. polymorpha* U and V gametologs was smaller than that between either gametolog and the ortholog in the other species indicated. Ingroup sequences (solid circles) were defined as orthologs whose sequence divergence from one of the *M. polymorpha* gametologs was smaller than the divergence between the two *M. polymorpha* gametologs, indicating divergence after the *M. polymorpha* U-V gametolog split. Specific designations of each ortholog as either U or V gametolog related are presented in Data S1C. See Data S2 and Figure 4 for phylogenetic trees of each of the gametologs. For the Marchantiopsida and Jungermanniopsida, we included only dioicous species where the transcriptome (*) or genome (°) was apparently derived from a single sex (i.e., where only single orthologs were detected for all the genes that we infer to be in the oldest evolutionary stratum [shaded purple]). Predicted nodes of the origins (color coded) of the non-recombining regions of the *M. polymorpha* U and V chromosomes are indicated on the chromosome schematic and the presently accepted liverwort phylogenetic tree (above the matrix).[35,36] Geologic ages of numbered nodes as previously estimated[37,38] are listed at left of the tree. See also Data S1A, S1C, and S2.

Jungermanniopsida and other Marchantiopsida sequences. These analyses suggest that the *M. polymorpha* U and V chromosomes consist of a mosaic of at least five evolutionary strata, with 7 pairs of "ancient" gametologs, including *BPCU* and *BPCV*, pre-dating the divergence of extant liverworts (purple horizontal regions in Figure 5). Other possible strata can be defined based on the other patterns of *M. polymorpha* U and V gametolog divergence relative to orthologs from other liverwort species (Figure 4; Data S2; see the Figure 5 legend). No pseudoautosomal regions were identified.

DISCUSSION

The chromosome level assemblies of the *M. polymorpha* U and V[20] chromosomes allow a test of the theoretical predictions that UV sex chromosomes should evolve symmetrically[14] and that both should show minimal degeneration.[23] While the *M. polymorpha* U and V chromosomes have evolved symmetrically, the low gene numbers (<5% of each autosome) suggest that they have undergone substantial degeneration.[19–21] The low gene density is consistent with this, as repetitive sequence accumulation can occur if there are few genes.[19–21] No obvious synteny is detectable between the U and V chromosomes, and the evolutionary strata inferred are not contiguous, implying that each sex chromosome has undergone independent chromosomal rearrangements.

Our results demonstrate that a U-linked transcription factor gene, *BPCU*, is the sex determinant *Feminizer* in *M. polymorpha*. Unexpectedly, however, *BPCU* is also essential for reproductive induction in females, a function which, in males, is carried out by its gametolog on the V chromosome, *BPCV*. The conserved function in the reproductive transition of both *BPCU* and *BPCV* suggests that this presumably ancestral function was retained despite only *BPCU* evolved a sex-determining (feminizing) function promoting female organ development (Figure 6). That *BPCU* and *BPCV* have apparently equivalent, and required, roles in the reproductive transition explains why the originally isolated *bpcU* mutants were aneuploid, with *BPCV* enabling the transition to reproductive development in the *bpcU* [UV] background.

Including *BPCU* and *BPCV*, seven ancient gametolog pairs are present on the *M. polymorpha* sex chromosomes, implying that large non-recombining regions were already established in the ancestral liverwort, which is estimated to have existed in the Mid-Silurian, ca. 430 mya. This age precedes any other known sex chromosome system. The oldest XY and ZW angiosperm sex chromosomes evolved in the Cenozoic (30–40 mya),[9] the U/V sex chromosome systems in green[39] and brown algae[40]

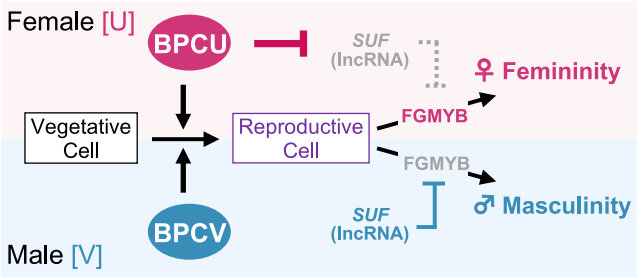

Figure 6. Genetic model of feminization by BPCU and reproductive induction by BPCU and BPCV

The female and male plants carry *BPCU* on the U chromosome and *BPCV* on the V chromosome, respectively. *BPCU* and *BPCV* share a function involved in inducing sexual reproduction. Following the transition to reproductive development, the female thallus initiates expression of the transcription factor FGMYB that promotes development of female reproductive organs. In gametophytes that do not carry *BPCU*, expression of the antisense long noncoding (lnc) RNA *SUF* prevents *FGMYB* expression, leading to male reproductive development. The U-linked *Feminizer*, *BPCU* functions to repress antisense *SUF* expression in females, allowing *FGMYB* expression and leading to female reproductive development.

arose in the Cretaceous (75 and 110 mya, respectively), and the mammalian X and Y chromosomes date to the Jurassic (180 mya).[41] The oldest previously described UV sex chromosomes of the moss *C. purpureus* evolved in the Carboniferous (300 mya),[23] and even the oldest mating-type system known thus far, pheromone receptor alleles in *Microbotryum* fungal species, has been dated to the Devonian (370 mya).[42]

Relative to *BPCU* and *BPCV*, each of the other six ancient pairs of gametologs has experienced recombination either between the sex chromosomes, or between a sex chromosome and an autosome, in various liverwort lineages (Figure 5). These data are consistent with the possibility that *BPCU* acted as the *Feminizer* in the ancestral liverwort. Given that *FGMYB* orthologs promote female gametophyte development in both *M. polymorpha* and *Arabidopsis thaliana*,[43] it probably promoted female gametophyte development in the common ancestor of land plants. In extant *M. polymorpha*, *FGMYB* acts as a binary switch, resulting in female differentiation when it is active, with differentiation as males as a "default" when *FGMYB* is repressed.[43] The genetic pathway(s) promoting maleness are as yet unknown. It is thus of interest whether the *BPCU* and *FGMYB*/*SUF* regulatory module is conserved in other liverworts and other bryophyte lineages with sex chromosomes (Figure 6). While there is no solid evidence of liverwort gametologs diverging prior to extant liverwort divergence, this does not preclude an earlier origin of dioicy, a condition possibly present in the ancestral land plant.

One plausible scenario is that the ancestral *BPC* gene functioned in the transition from vegetative to reproductive growth, and in the ancestral liverwort, an allele of *BPC* acquired a role in specifying female sex organ development, perhaps via its regulation of *FGMYB*. This allele evolved into *BPCU*, while the alternative allele (now the gametolog), *BPCV*, retained the ancestral function in the reproductive transition but did not acquire a sex-determining function. This can potentially explain the fact that, in addition to its role in sex determination, *BPCU* functions in the initiation of reproductive development, like its gametolog *BPCV*. This scenario is distinct from that described for other sex-determining systems. For example, in therian mammals, the male sex determinant *SRY* does not share the non-sex determination function of its X-linked gametolog, *SOX3*, which was presumably retained from the common ancestral gene.[44] Likewise, the sex determinant *MID* in the chlorophyte alga *Volvox carteri* evolved directly from an already male-specific gene within the ancestral mating-type locus.[33] Our findings provide a distinct trajectory for the evolution of a sex determinant (the *Feminizer*) in another haploid system and further implies that a pair of gametologs that initially appear functionally equivalent may have been differentiated to serve females and males unequally.

STAR★METHODS

Detailed methods are provided in the online version of this paper and include the following:

- KEY RESOURCES TABLE
- RESOURCE AVAILABILITY
  - Lead contact
  - Materials availability
  - Data and code availability
- EXPERIMENTAL MODEL AND SUBJECT DETAILS
  - Plant materials and culture
- METHOD DETAILS
  - Plant transformation
  - U chromosome assembly
  - Genetic nomenclature
  - Microscopy
  - RNA extraction and reverse-transcription
  - Plasmid construction for expressing BPCU and BPCV
  - Genome editing
  - Genotyping and sex diagnosis
  - Generation of transgenic lines expressing genomic BPCU and genomic BPCV
  - RT-PCR
  - Quantitative real-time RT-PCR
  - DPI-ELISA with BPCU and selected DNA-probes
  - Flow cytometry analysis
  - Chromatin profiling analysis
  - Analysis of sex chromosome evolution
  - Data analysis of CUT&RUN
  - Transcriptome Mapping
- QUANTIFICATION AND STATISTICAL ANALYSIS
  - General statistical analyses
  - Gene expression analysis of BPCU and BPCV

SUPPLEMENTAL INFORMATION

Supplemental information can be found online at https://doi.org/10.1016/j.cub.2021.10.023.

ACKNOWLEDGMENTS

Authors thank Qi Zhou for critical reading of the manuscript, Aino Komatsu for isolation of the segregated plants with both U and V chromosomes, and Keitaro Okahashi for initial contribution to select candidate genes. Computations were performed on the NIG supercomputer at ROIS National Institute of Genetics, the supercomputer of ACCMS at Kyoto University, and the supercomputer of the HPC Computing Center at Kindai University. We thank Takefumi

Kondo and Yukari Sando (NGS core facility of Graduate School of Biostudies, Kyoto University) for supporting the RNA sequencing (RNA-seq) analysis. Research was funded by JSPS/MEXT KAKENHI, grant numbers: JP17H07424 and JP19H05675 to T. Kohchi, 20510185 and 24510272 to K.T.Y., JP20H05780 to S.Y., JP20K15783 to Y.T., JP16H06279 (PAGS) to Y.N., JP19K16166 to Y. Yoshitake, and JP19K16167 to Y. Yasui. T. Kohchi was also supported by JSPS Bilateral Joint Research Projects JPJSBP120192003. D.W. was supported by the German Research Foundation (DFG; WA2814/4-1). C.L. was supported by European Research Council under the European Union's Horizon 2020 research and innovation programme 757600. F.B. was supported by the Gregor Mendel Institute (FB) and FWF international cooperation grant I4258. S.A.M. was supported by the FWF grant DK1238 chromosome dynamics. J.L.B. was supported by Australian Research Council DP200100225.

AUTHOR CONTRIBUTIONS

M.I. and T. Kajiwara performed a majority of the experiments by the help and supervision of Y. Yasui, Y. Yoshitake, M.M., N.S., R.N., S.Y., and T. Kohchi. Y. Yoshitake, T. Kajiwara, S.K., and S.A.M. performed CUT&RUN assays and RNA-seq analyses. S.A.M., Y.T., C.L., K.T.Y., and F.B. performed chromosome assembly. M.Y., T.M., M.S., and Y.T. performed genome annotation and constructed the genome database under the supervision of Y.N. S.S. and J.L.B. performed bioinformatic analysis on sex chromosome evolution. D.W., K.H., and K.K. performed DNA binding experiments. T. Kohchi, F.B., J.L.B., and K.T.Y. designed the project and contributed to conceptualize the work. T. Kohchi, K.T.Y., F.B., and J.L.B. wrote the manuscript with input from all authors. All authors jointly interpreted the data and thoroughly checked the manuscript.

DECLARATION OF INTERESTS

The authors declare no competing interests.

Received: June 7, 2021
Revised: August 2, 2021
Accepted: October 8, 2021
Published: November 3, 2021

REFERENCES

1. Bachtrog, D., Kirkpatrick, M., Mank, J.E., McDaniel, S.F., Pires, J.C., Rice, W., and Valenzuela, N. (2011). Are all sex chromosomes created equal? Trends Genet. *27*, 350–357.
2. Akagi, T., and Charlesworth, D. (2019). Pleiotropic effects of sex-determining genes in the evolution of dioecy in two plant species. Proc. R. Soc. B: Biol. Sci. *286*, 20191805.
3. Akagi, T., Henry, I.M., Tao, R., and Comai, L. (2014). Plant genetics. A Y-chromosome-encoded small RNA acts as a sex determinant in persimmons. Science *346*, 646–650.
4. Boualem, A., Troadec, C., Camps, C., Lemhemdi, A., Morin, H., Sari, M.A., Fraenkel-Zagouri, R., Kovalski, I., Dogimont, C., Perl-Treves, R., and Bendahmane, A. (2015). A cucurbit androecy gene reveals how unisexual flowers develop and dioecy emerges. Science *350*, 688–691.
5. Müller, N.A., Kersten, B., Leite Montalvão, A.P., Mähler, N., Bernhardsson, C., Bräutigam, K., Carracedo Lorenzo, Z., Hoenicka, H., Kumar, V., Mader, M., et al. (2020). A single gene underlies the dynamic evolution of poplar sex determination. Nat. Plants *6*, 630–637.
6. Akagi, T., Pilkington, S.M., Varkonyi-Gasic, E., Henry, I.M., Sugano, S.S., Sonoda, M., Firl, A., McNeilage, M.A., Douglas, M.J., Wang, T., et al. (2019). Two Y-chromosome-encoded genes determine sex in kiwifruit. Nat. Plants *5*, 801–809.
7. Harkess, A., Huang, K., van der Hulst, R., Tissen, B., Caplan, J.L., Koppula, A., Batish, M., Meyers, B.C., and Leebens-Mack, J. (2020). Sex determination by two Y-linked genes in garden asparagus. Plant Cell *32*, 1790–1796.
8. Charlesworth, B., and Charlesworth, D. (1978). Model for evolution of dioecy and gynodioecy. Am. Nat. *112*, 975–997.
9. Renner, S.S., and Müller, N.A. (2021). Plant sex chromosomes defy evolutionary models of expanding recombination suppression and genetic degeneration. Nat. Plants *7*, 392–402.
10. Coelho, S.M., Gueno, J., Lipinska, A.P., Cock, J.M., and Umen, J.G. (2018). UV chromosomes and haploid sexual systems. Trends Plant Sci. *23*, 794–807.
11. Coelho, S.M., Mignerot, L., and Cock, J.M. (2019). Origin and evolution of sex-determination systems in the brown algae. New Phytol. *222*, 1751–1756.
12. Higo, A., Kawashima, T., Borg, M., Zhao, M., López-Vidriero, I., Sakayama, H., Montgomery, S.A., Sekimoto, H., Hackenberg, D., Shimamura, M., et al. (2018). Transcription factor DUO1 generated by neo-functionalization is associated with evolution of sperm differentiation in plants. Nat. Commun. *9*, 5283.
13. Liu, X., Bogaert, K., Engelen, A.H., Leliaert, F., Roleda, M.Y., and De Clerck, O. (2017). Seaweed reproductive biology: environmental and genetic controls. Bot. Mar. *60*, 89–108.
14. Bull, J.J. (1978). Sex chromosomes in haploid dioecy: a unique contrast to Muller's theory for diploid dioecy. Am. Nat. *112*, 245–250.
15. Lewis, K.R. (1961). The genetics of bryophytes. T. Brit. Bryol. Soc. *4*, 111–130.
16. Bachtrog, D., Mank, J.E., Peichel, C.L., Kirkpatrick, M., Otto, S.P., Ashman, T.L., Hahn, M.W., Kitano, J., Mayrose, I., Ming, R., et al.; Tree of Sex Consortium (2014). Sex determination: why so many ways of doing it? PLoS Biol. *12*, e1001899.
17. Bull, J.J. (1983). Evolution of Sex Determining Mechanisms (The Benjamin/Cummings Publishing Company).
18. Bowman, J.L. (2016). A brief history of *Marchantia* from Greece to genomics. Plant Cell Physiol. *57*, 210–229.
19. Bowman, J.L., Kohchi, T., Yamato, K.T., Jenkins, J., Shu, S., Ishizaki, K., Yamaoka, S., Nishihama, R., Nakamura, Y., Berger, F., et al. (2017). Insights into land plant evolution garnered from the *Marchantia polymorpha* genome. Cell *171*, 287–304.e15.
20. Montgomery, S.A., Tanizawa, Y., Galik, B., Wang, N., Ito, T., Mochizuki, T., Akimcheva, S., Bowman, J.L., Cognat, V., Maréchal-Drouard, L., et al. (2020). Chromatin organization in early land plants reveals an ancestral association between H3K27me3, transposons, and constitutive heterochromatin. Curr. Biol. *30*, 573–588.e7.
21. Yamato, K.T., Ishizaki, K., Fujisawa, M., Okada, S., Nakayama, S., Fujishita, M., Bando, H., Yodoya, K., Hayashi, K., Bando, T., et al. (2007). Gene organization of the liverwort Y chromosome reveals distinct sex chromosome evolution in a haploid system. Proc. Natl. Acad. Sci. USA *104*, 6472–6477.
22. Haupt, G. (1932). Beiträge zur Zytologie der Gattung Marchantia (L.). I. Zeitschr. Ind. Abst. Vererbungsl. *62*, 367–428.
23. Carey, S.B., Jenkins, J., Lovell, J.T., Maumus, F., Sreedasyam, A., Payton, A.C., Shu, S., Tiley, G.P., Fernandez-Pozo, N., Healey, A., et al. (2021). Gene-rich UV sex chromosomes harbor conserved regulators of sexual development. Sci. Adv. *7*, eabh2488.
24. Silva, A.T., Gao, B., Fisher, K.M., Mishler, B.D., Ekwealor, J.T.B., Stark, L.R., Li, X., Zhang, D., Bowker, M.A., Brinda, J.C., et al. (2021). To dry perchance to live: insights from the genome of the desiccation-tolerant biocrust moss *Syntrichia caninervis*. Plant J. *105*, 1339–1356.
25. Ahmed, S., Cock, J.M., Pessia, E., Luthringer, R., Cormier, A., Robuchon, M., Sterck, L., Peters, A.F., Dittami, S.M., Corre, E., et al. (2014). A haploid system of sex determination in the brown alga Ectocarpus sp. Curr. Biol. *24*, 1945–1957.
26. Lieberman-Aiden, E., van Berkum, N.L., Williams, L., Imakaev, M., Ragoczy, T., Telling, A., Amit, I., Lajoie, B.R., Sabo, P.J., Dorschner, M.O., et al. (2009). Comprehensive mapping of long-range interactions reveals folding principles of the human genome. Science *326*, 289–293.

27. Nakayama, S., Fujishita, M., Sone, T., and Ohyama, K. (2001). Additional locus of rDNA sequence specific to the X chromosome of the liverwort, *Marchantia polymorpha*. Chromosome Res. *9*, 469–473.

28. Hisanaga, T., Okahashi, K., Yamaoka, S., Kajiwara, T., Nishihama, R., Shimamura, M., Yamato, K.T., Bowman, J.L., Kohchi, T., and Nakajima, K. (2019). A *cis*-acting bidirectional transcription switch controls sexual dimorphism in the liverwort. EMBO J. *38*, 663–669.

29. Thorvaldsdóttir, H., Robinson, J.T., and Mesirov, J.P. (2013). Integrative Genomics Viewer (IGV): high-performance genomics data visualization and exploration. Brief. Bioinform. *14*, 178–192.

30. Zang, C., Schones, D.E., Zeng, C., Cui, K., Zhao, K., and Peng, W. (2009). A clustering approach for identification of enriched domains from histone modification ChIP-seq data. Bioinformatics *25*, 1952–1958.

31. Sangwan, I., and O'Brian, M.R. (2002). Identification of a soybean protein that interacts with GAGA element dinucleotide repeat DNA. Plant Physiol. *129*, 1788–1794.

32. Theune, M.L., Bloss, U., Brand, L.H., Ladwig, F., and Wanke, D. (2019). Phylogenetic analyses and GAGA-motif binding studies of BBR/BPC proteins lend to clues in GAGA-motif recognition and a regulatory role in brassinosteroid signaling. Front. Plant Sci. *10*, 466.

33. Geng, S., De Hoff, P., and Umen, J.G. (2014). Evolution of sexes from an ancestral mating-type specification pathway. PLoS Biol. *12*, e1001904.

34. Li, F.W., Nishiyama, T., Waller, M., Frangedakis, E., Keller, J., Li, Z., Fernandez-Pozo, N., Barker, M.S., Bennett, T., Blázquez, M.A., et al. (2020). Anthoceros genomes illuminate the origin of land plants and the unique biology of hornworts. Nat. Plants *6*, 259–272.

35. Forrest, L.L., Davis, E.C., Long, D.G., Crandall-Stotler, B.J., Clark, A., and Hollingsworth, M.L. (2006). Unraveling the evolutionary history of the liverworts (Marchantiophyta): multiple taxa, genomes and analyses. Bryologist *109*, 303–334.

36. He-Nygrén, X., Juslén, A., Ahonen, I., Glenny, D., and Piippo, S. (2006). Illuminating the evolutionary history of liverworts (Marchantiophyta) - towards a natural classification. Cladistics *22*, 1–31.

37. Morris, J.L., Puttick, M.N., Clark, J.W., Edwards, D., Kenrick, P., Pressel, S., Wellman, C.H., Yang, Z., Schneider, H., and Donoghue, P.C.J. (2018). The timescale of early land plant evolution. Proc. Natl. Acad. Sci. USA *115*, E2274–E2283.

38. Villarreal A, J.C., Crandall-Stotler, B.J., Hart, M.L., Long, D.G., and Forrest, L.L. (2016). Divergence times and the evolution of morphological complexity in an early land plant lineage (Marchantiopsida) with a slow molecular rate. New Phytol. *209*, 1734–1746.

39. Yamamoto, K., Hamaji, T., Kawai-Toyooka, H., Matsuzaki, R., Takahashi, F., Nishimura, Y., Kawachi, M., Noguchi, H., Minakuchi, Y., Umen, J.G., et al. (2021). Three genomes in the algal genus *Volvox* reveal the fate of a haploid sex-determining region after a transition to homothallism. Proc. Natl. Acad. Sci. USA *118*, e2100712118.

40. Lipinska, A.P., Toda, N.R.T., Heesch, S., Peters, A.F., Cock, J.M., and Coelho, S.M. (2017). Multiple gene movements into and out of haploid sex chromosomes. Genome Biol. *18*, 104.

41. Hughes, J.F., and Page, D.C. (2015). The biology and evolution of mammalian Y chromosomes. Annu. Rev. Genet. *49*, 507–527.

42. Devier, B., Aguileta, G., Hood, M.E., and Giraud, T. (2009). Ancient trans-specific polymorphism at pheromone receptor genes in basidiomycetes. Genetics *181*, 209–223.

43. Hisanaga, T., Yamaoka, S., Kawashima, T., Higo, A., Nakajima, K., Araki, T., Kohchi, T., and Berger, F. (2019). Building new insights in plant gametogenesis from an evolutionary perspective. Nat. Plants *5*, 663–669.

44. Katsura, Y., Kondo, H.X., Ryan, J., Harley, V., and Satta, Y. (2018). The evolutionary process of mammalian sex determination genes focusing on marsupial SRYs. BMC Evol. Biol. *18*, 3.

45. Deblaere, R., Bytebier, B., De Greve, H., Deboeck, F., Schell, J., Van Montagu, M., and Leemans, J. (1985). Efficient octopine Ti plasmid-derived vectors for Agrobacterium-mediated gene transfer to plants. Nucleic Acids Res. *13*, 4777–4788.

46. Gamborg, O.L., Miller, R.A., and Ojima, K. (1968). Nutrient requirements of suspension cultures of soybean root cells. Exp. Cell Res. *50*, 151–158.

47. Pluthero, F.G. (1993). Rapid purification of high-activity Taq DNA polymerase. Nucleic Acids Res. *21*, 4850–4851.

48. Skene, P.J., and Henikoff, S. (2017). An efficient targeted nuclease strategy for high-resolution mapping of DNA binding sites. eLife *6*, e21856.

49. Higo, A., Niwa, M., Yamato, K.T., Yamada, L., Sawada, H., Sakamoto, T., Kurata, T., Shirakawa, M., Endo, M., Shigenobu, S., et al. (2016). Transcriptional framework of male gametogenesis in the liverwort *Marchantia polymorpha* L. Plant Cell Physiol. *57*, 325–338.

50. Yamaoka, S., Nishihama, R., Yoshitake, Y., Ishida, S., Inoue, K., Saito, M., Okahashi, K., Bao, H., Nishida, H., Yamaguchi, K., et al. (2018). Generative cell specification requires transcription factors evolutionarily conserved in land plants. Curr. Biol. *28*, 479–486.e5.

51. Ishizaki, K., Nishihama, R., Ueda, M., Inoue, K., Ishida, S., Nishimura, Y., Shikanai, T., and Kohchi, T. (2015). Development of gateway binary vector series with four different selection markers for the liverwort *Marchantia polymorpha*. PLoS ONE *10*, e0138876.

52. Sugano, S.S., Nishihama, R., Shirakawa, M., Takagi, J., Matsuda, Y., Ishida, S., Shimada, T., Hara-Nishimura, I., Osakabe, K., and Kohchi, T. (2018). Efficient CRISPR/Cas9-based genome editing and its application to conditional genetic analysis in *Marchantia polymorpha*. PLoS ONE *13*, e0205117.

53. Koide, E., Suetsugu, N., Iwano, M., Gotoh, E., Nomura, Y., Stolze, S.C., Nakagami, H., Kohchi, T., and Nishihama, R. (2020). Regulation of photosynthetic carbohydrate metabolism by a Raf-like kinase in the liverwort *Marchantia polymorpha*. Plant Cell Physiol. *61*, 631–643.

54. Chen, S., Zhou, Y., Chen, Y., and Gu, J. (2018). fastp: an ultra-fast all-in-one FASTQ preprocessor. Bioinformatics *34*, i884–i890.

55. Patro, R., Duggal, G., Love, M.I., Irizarry, R.A., and Kingsford, C. (2017). Salmon provides fast and bias-aware quantification of transcript expression. Nat. Methods *14*, 417–419.

56. Langmead, B., and Salzberg, S.L. (2012). Fast gapped-read alignment with Bowtie 2. Nat. Methods *9*, 357–359.

57. Dobin, A., Davis, C.A., Schlesinger, F., Drenkow, J., Zaleski, C., Jha, S., Batut, P., Chaisson, M., and Gingeras, T.R. (2013). STAR: ultrafast universal RNA-seq aligner. Bioinformatics *29*, 15–21.

58. Danecek, P., Bonfield, J.K., Liddle, J., Marshall, J., Ohan, V., Pollard, M.O., Whitwham, A., Keane, T., McCarthy, S.A., Davies, R.M., and Li, H. (2021). Twelve years of SAMtools and BCFtools. GigaScience *10*, giab008.

59. Ramírez, F., Ryan, D.P., Grüning, B., Bhardwaj, V., Kilpert, F., Richter, A.S., Heyne, S., Dündar, F., and Manke, T. (2016). deepTools2: a next generation web server for deep-sequencing data analysis. Nucleic Acids Res. *44* (W1), W160–W165.

60. Soneson, C., Love, M.I., and Robinson, M.D. (2015). Differential analyses for RNA-seq: transcript-level estimates improve gene-level inferences. F1000Res. *4*, 1521.

61. Ruan, J., and Li, H. (2020). Fast and accurate long-read assembly with wtdbg2. Nat. Methods *17*, 155–158.

62. Hu, J., Fan, J., Sun, Z., and Liu, S. (2020). NextPolish: a fast and efficient genome polishing tool for long-read assembly. Bioinformatics *36*, 2253–2255.

63. Walker, B.J., Abeel, T., Shea, T., Priest, M., Abouelliel, A., Sakthikumar, S., Cuomo, C.A., Zeng, Q., Wortman, J., Young, S.K., and Earl, A.M. (2014). Pilon: an integrated tool for comprehensive microbial variant detection and genome assembly improvement. PLoS ONE *9*, e112963.

64. Dudchenko, O., Batra, S.S., Omer, A.D., Nyquist, S.K., Hoeger, M., Durand, N.C., Shamim, M.S., Machol, I., Lander, E.S., Aiden, A.P., and Aiden, E.L. (2017). De novo assembly of the *Aedes aegypti* genome using Hi-C yields chromosome-length scaffolds. Science *356*, 92–95.

65. Wu, T.D., and Watanabe, C.K. (2005). GMAP: a genomic mapping and alignment program for mRNA and EST sequences. Bioinformatics *21*, 1859–1875.

66. Huelsenbeck, J.P., and Ronquist, F. (2001). MRBAYES: Bayesian inference of phylogenetic trees. Bioinformatics *17*, 754–755.

67. Huelsenbeck, J.P., Ronquist, F., Nielsen, R., and Bollback, J.P. (2001). Bayesian inference of phylogeny and its impact on evolutionary biology. Science *294*, 2310–2314.

68. Korber, B. (2000). HIV signature and sequence variation analysis. In Computational Analysis of HIV Molecular Sequences, A.G. Rodrigo, and G.H. Learn, Jr., eds. (Kluwer Academic), pp. 55–72.

69. Chiyoda, S., Linley, P.J., Yamato, K.T., Fukuzawa, H., Yokota, A., and Kohchi, T. (2007). Simple and efficient plastid transformation system for the liverwort *Marchantia polymorpha* L. suspension-culture cells. Transgenic Res. *16*, 41–49.

70. Ishizaki, K., Nishihama, R., Yamato, K.T., and Kohchi, T. (2016). Molecular genetic tools and techniques for *Marchantia polymorpha* research. Plant Cell Physiol. *57*, 262–270.

71. Kubota, A., Kita, S., Ishizaki, K., Nishihama, R., Yamato, K.T., and Kohchi, T. (2014). Co-option of a photoperiodic growth-phase transition system during land plant evolution. Nat. Commun. *5*, 3668.

72. Ishizaki, K., Chiyoda, S., Yamato, K.T., and Kohchi, T. (2008). *Agrobacterium*-mediated transformation of the haploid liverwort *Marchantia polymorpha* L., an emerging model for plant biology. Plant Cell Physiol. *49*, 1084–1091.

73. Kubota, A., Ishizaki, K., Hosaka, M., and Kohchi, T. (2013). Efficient *Agrobacterium*-mediated transformation of the liverwort *Marchantia polymorpha* using regenerating thalli. Biosci. Biotechnol. Biochem. *77*, 167–172.

74. Bowman, J.L., Araki, T., Arteaga-Vazquez, M.A., Berger, F., Dolan, L., Haseloff, J., Ishizaki, K., Kyozuka, J., Lin, S.S., Nagasaki, H., et al. (2016). The naming of names: guidelines for gene nomenclature in *Marchantia*. Plant Cell Physiol. *57*, 257–261.

75. Ishizaki, K., Mizutani, M., Shimamura, M., Masuda, A., Nishihama, R., and Kohchi, T. (2013). Essential role of the E3 ubiquitin ligase nopperabo1 in schizogenous intercellular space formation in the liverwort *Marchantia polymorpha*. Plant Cell *25*, 4075–4084.

76. Fujisawa, M., Hayashi, K., Nishio, T., Bando, T., Okada, S., Yamato, K.T., Fukuzawa, H., and Ohyama, K. (2001). Isolation of X and Y chromosome-specific DNA markers from a liverwort, *Marchantia polymorpha*, by representational difference analysis. Genetics *159*, 981–985.

77. Inoue, K., Nishihama, R., Kataoka, H., Hosaka, M., Manabe, R., Nomoto, M., Tada, Y., Ishizaki, K., and Kohchi, T. (2016). Phytochrome signaling is mediated by PHYTOCHROME INTERACTING FACTOR in the liverwort *Marchantia polymorpha*. Plant Cell *28*, 1406–1421.

78. Livak, K.J., and Schmittgen, T.D. (2001). Analysis of relative gene expression data using real-time quantitative PCR and the 2(-Delta Delta C(T)) method. Methods *25*, 402–408.

79. Brand, L.H., Kirchler, T., Hummel, S., Chaban, C., and Wanke, D. (2010). DPI-ELISA: a fast and versatile method to specify the binding of plant transcription factors to DNA in vitro. Plant Methods *6*, 25.

80. Fischer, S.M., Böser, A., Hirsch, J.P., and Wanke, D. (2016). Quantitative analysis of protein-DNA interaction by qDPI-ELISA. Methods Mol. Biol. *1482*, 49–66.

81. Nishihama, R., Ishizaki, K., Hosaka, M., Matsuda, Y., Kubota, A., and Kohchi, T. (2015). Phytochrome-mediated regulation of cell division and growth during regeneration and sporeling development in the liverwort Marchantia polymorpha. J. Plant Res. *128*, 407–421.

82. Dong, S., Zhao, C., Zhang, S., Wu, H., Mu, W., Wei, T., Li, N., Wan, T., Liu, H., Cui, J., et al. (2019). The amount of RNA editing sites in liverwort organellar genes is correlated with GC content and nuclear PPR protein diversity. Genome Biol. Evol. *11*, 3233–3239.

83. Leebens-Mack, J.H., Barker, M.S., Carpenter, E.J., Deyholos, M.K., Gitzendanner, M.A., Graham, S.W., Grosse, I., Li, Z., Melkonian, M., Mirarab, S., et al.; One Thousand Plant Transcriptomes Initiative (2019). One thousand plant transcriptomes and the phylogenomics of green plants. Nature *574*, 679–685.

84. Linde, A.M., Sawangproh, W., Cronberg, N., Szövényi, P., and Lagercrantz, U. (2020). Evolutionary history of the *Marchantia polymorpha* complex. Front. Plant Sci. *11*, 829.

85. Radhakrishnan, G.V., Keller, J., Rich, M.K., Vernié, T., Mbadinga Mbadinga, D.L., Vigneron, N., Cottret, L., Clemente, H.S., Libourel, C., Cheema, J., et al. (2020). An ancestral signalling pathway is conserved in intracellular symbioses-forming plant lineages. Nat. Plants *6*, 280–289.

86. Wickett, N.J., Mirarab, S., Nguyen, N., Warnow, T., Carpenter, E., Matasci, N., Ayyampalayam, S., Barker, M.S., Burleigh, J.G., Gitzendanner, M.A., et al. (2014). Phylotranscriptomic analysis of the origin and early diversification of land plants. Proc. Natl. Acad. Sci. USA *111*, E4859–E4868.

87. Nei, M., and Gojobori, T. (1986). Simple methods for estimating the numbers of synonymous and nonsynonymous nucleotide substitutions. Mol. Biol. Evol. *3*, 418–426.

STAR★METHODS

KEY RESOURCES TABLE

REAGENT or RESOURCE	SOURCE	IDENTIFIER
Antibodies		
Rabbit polyclonal H3	Abcam	Cat# ab1791; RRID: AB_302613
Rabbit polyclonal H3K27me3	Millipore	Cat# 07-449; RRID: AB_310624
HRP Anti-6X His tag antibody	Abcam	Cat# ab1187, RRID: AB_298652
Bacterial and virus strains		
Escherichia coli DH5a	Widely distributed	N/A
Agrobacterium tumefaciens GV2260	Deblaere et al.[45]	N/A
Escherichia coli BL21-CodonPlus-RIL	Agilent	Cat# 230240
Biological samples		
HEK293 DNA	Danhua Jiang, Beijing, China	N/A
Chemicals, peptides, and recombinant proteins		
Gamborg's B5 salts	Gamborg et al.[46]	N/A
HYPONeX	Hyponex Japan	Cat# 4977517180036
hygromycin B	Nacalai Tesque	Cat# 07296-24
cefotaxime (CLAFORAN)	Sanofi	Cat# 6132409D1050
TRIzol reagent	ThermoFisher Scientific	Cat# 15596018
ReverTra Ace	Toyobo Life Science	Cat# TRT-101
RNase A	ThermoFisher Scientific	Cat# EN0531
RNase A	Sigma-Aldrich	Cat# R5125
RQ1 RNase-Free DNase	Promega	Cat# M610A
Proteinase K	Thermo Fisher Scientific	Cat# EO0491
Taq DNA polymerase	Pluthero[47]	N/A
Bio-Mag Plus Concanavalin A coated beads	polysciences	Cat# 86057
cOmplete Protease Inhibitor Cocktail	Roche	Cat# 11697498001
pA-MNase	Skene and Henikoff[48]	Henikoff lab batch #6 purified 11.01.2017
propidium iodide	Nacalai Tesque	Cat# 29037-76
ortho-phenylenediamine (OPD)	Merck-Sigma/Aldrich	Cat# P5412
sulfuric acid (2 N H_2SO_4)	Roth	Cat# 2609.1
SYBR Green Nucleic Acid Gel Stain	Lonza	Cat# 50513
Critical commercial assays		
KOD FX Neo DNA polymerase	Toyobo Life Science	Cat# KFX-201
KOD One PCR Master Mix	Toyobo Life Science	Cat# KMM-101
pENTR/D-TOPO Cloning kit	Thermo Fisher Scientific	Cat# K240020
Gateway LR clonase II Enzyme mix	Thermo Fisher Scientific	Cat# 11791020
NucleoSpin Gel and PCR Clean-up Kit	Macherey & Nagel	Cat# 740609.50
Pre-blocked clear flat-bottom Streptavidin Coated Plates (96-wells)	Pierce Thermo Fischer Scientific	Cat# 15124
Penta·His HRP Conjugate Kit	QIAGEN	Cat# 34460
Deposited data		
Marchantia polymorpha genome v3.1	Bowman et al.[19]	https://marchantia.info; SRA: SRR1800537
Marchantia polymorpha genome v5.1	Montgomery et al.[20]	https://marchantia.info; SRA: PRJNA553138
Marchantia polymorpha genome v6.1	This paper	https://marchantia.info; SRA: PRJDB11173
Iso-seq and RNA-seq for gene annotations	Montgomery et al.[20]	SRA: PRJDB8530 and PRJNA251267
Tak-1 thallus CUT&RUN	Montgomery et al.[20]	SRA: PRJNA553138

(*Continued on next page*)

Continued

REAGENT or RESOURCE	SOURCE	IDENTIFIER
Tak-2 and *bpcU* thallus CUT&RUN	This paper	SRA: PRJNA757234
Tak-1, Tak-2 and *bpcU* thallus RNA-seq	This paper	SRA: PRJNA757569
RNA-seq for expression analyses in various tissues	Bowman et al.,[19] Higo et al.,[49] and Yamaoka et al.[50]	SRA: DRR050351-53; DRR050346-48; DRR118943-45; DRR118949-51; SRR4450260-62; SRR4450254-56
Experimental models: Organisms/strains		
Marchantia polymorpha Tak-1	Bowman et al.[19]	N/A
Marchantia polymorpha Tak-2	Bowman et al.[19]	N/A
Marchantia polymorpha BC3-38	Yamaoka et al.[50]	N/A
Marchantia polymorpha UV plant	This paper	N/A
Marchantia polymorpha bpcU-101	This paper	N/A
Marchantia polymorpha bpcU-102	This paper	N/A
Marchantia polymorpha gBPCU$^{\#3}$	This paper	N/A
Marchantia polymorpha gBPCU$^{\#4}$	This paper	N/A
Marchantia polymorpha gBPCU$^{\#4}$ *fgmyb-31*	This paper	N/A
Marchantia polymorpha gBPCU$^{\#4}$ *fgmyb-41*	This paper	N/A
Marchantia polymorpha bpcU-1	This paper	N/A
Marchantia polymorpha bpcU-2	This paper	N/A
Marchantia polymorpha bpcU-3	This paper	N/A
Marchantia polymorpha bpcV-1	This paper	N/A
Marchantia polymorpha bpcV-2	This paper	N/A
Marchantia polymorpha bpcV-3	This paper	N/A
Marchantia polymorpha gBPCU$^{\#2}$ *bpcU-1*	This paper	N/A
Marchantia polymorpha gBPCU$^{\#4}$ *bpcU-1*	This paper	N/A
Marchantia polymorpha gBPCU$^{\#6}$ *bpcU-1*	This paper	N/A
Marchantia polymorpha gBPCV$^{\#7}$ *bpcU-1*	This paper	N/A
Marchantia polymorpha gBPCV$^{\#8}$ *bpcU-1*	This paper	N/A
Marchantia polymorpha gBPCV$^{\#9}$ *bpcU-1*	This paper	N/A
Oligonucleotides		
See Table S1	This paper	N/A
Recombinant DNA		
pENTR D-TOPO	Thermo Fisher Scientific	Cat# 45-0218
BPCU gene pENTRdTOPO	This paper	N/A
BPCV gene pENTRdTOPO	This paper	N/A
pMpGWB101	Ishizaki et al.[51]	GenBank: LC057443
pMpGWB301	Ishizaki et al.[51]	GenBank: LC057517
BPCU gene pMpGWB101	This paper	N/A
BPCU gene pMpGWB301	This paper	N/A
BPCV gene pMpGWB301	This paper	N/A
pMpGE_En03	Sugano et al.[52]	GenBank: LC090755
pMpGE_En04	Koide et al.[53]	N/A
pBC-GE12	Koide et al.[53]	N/A
pBC-GE23	Koide et al.[53]	N/A
pBC-GE34	Koide et al.[53]	N/A
BPCU.1 gRNA pMpGE_En03	This paper	N/A
BPCU gRNALDs pMpGE_En04	This paper	N/A
BPCV.1 gRNA pMpGE_En03	This paper	N/A
BPCV.2 gRNA pMpGE_En03	This paper	N/A

(*Continued on next page*)

Continued

REAGENT or RESOURCE	SOURCE	IDENTIFIER
FGMYB gRNA3 pMpGE_En03	This paper	N/A
FGMYB gRNA4 pMpGE_En03	This paper	N/A
pMpGE010	Sugano et al.[52]	GenBank: LC090756
pMpGE011	Sugano et al.[52]	GenBank: LC090757
pMpGE017	Koide et al.[53]	N/A
BPCU.1 gRNA pMpGE010	This paper	N/A
BPCU gRNALDs pMpGE017	This paper	N/A
BPCV.1 gRNA pMpGE010	This paper	N/A
BPCV.2 gRNA pMpGE010	This paper	N/A
FGMYB gRNA3 pMpGE011	This paper	N/A
FGMYB gRNA4 pMpGE011	This paper	N/A
BPCU cds pENTRdTOPO	This paper	N/A
BPCV cds pENTRdTOPO	This paper	N/A
pET-DEST42	Thermo Fisher Scientific	Cat# 12276010
BPCU cds pET-DEST42	This paper	N/A
BPCV cds pET-DEST42	This paper	N/A
Software and algorithms		
fastp v0.20.1	Chen et al.[54]	https://github.com/OpenGene/fastp
Salmon v0.14.1	Patro et al.[55]	https://github.com/COMBINE-lab/salmon
bowtie2 v2.4.1	Langmead and Salzberg[56]	https://github.com/BenLangmead/bowtie2
STAR v2.7.3a	Dobin et al.[57]	https://github.com/alexdobin/STAR
samtools v1.9.0	Danecek et al.[58]	https://github.com/samtools/
deeptools v3.5.0	Ramírez et al.[59]	https://github.com/deeptools/deepTools
faCount	UCSC Genome Browser	https://hgdownload.cse.ucsc.edu/admin/exe/
SICER2	Zang et al.[30]	https://zanglab.github.io/SICER2/
tximport	Soneson et al.[60]	https://bioconductor.org/packages/release/bioc/html/tximport.html
IGV v2.8.0	Thorvaldsdóttir et al.[29]	https://software.broadinstitute.org/software/igv/
Redbean v2.5	Ruan and Li[61]	https://github.com/ruanjue/wtdbg2
NextPolish v1.3.1	Hu et al.[62]	https://github.com/Nextomics/NextPolish
Pilon v1.23	Walker et al.[63]	https://github.com/broadinstitute/pilon
NextDenovo v2.2-beta.0	GrandOmics	https://github.com/Nextomics/NextDenovo
3D-DNA pipeline	Dudchenko et al.[64]	https://github.com/aidenlab/3d-dna
GMAP ver. 2019.09.12	Wu and Watanabe[65]	http://research-pub.gene.com/gmap/
Se-Al v2.0a11	Institute of Evolutionary Biology University of Edinburgh	http://tree.bio.ed.ac.uk/software/seal/
MrBayes 3.2.1	Huelsenbeck and Ronquist[66] and Huelsenbeck et al.[67]	https://nbisweden.github.io/MrBayes/index.html
FigTree v1.4.0	Institute of Evolutionary Biology University of Edinburgh	http://tree.bio.ed.ac.uk/software/figtree/
SNAP v2.1.1	Korber[68]	https://hcv.lanl.gov/content/sequence/SNAP/SNAP.html
Other		
BD FACSARIA III	BD Biosciences	https://www.bdbiosciences.com/en-us
BD Accuri C6 Flow Cytometer	BD Biosciences	https://www.bdbiosciences.com/en-us
CFX96 real-time PCR detection system	Bio-Rad Laboratories	https://www.bio-rad.com
NanoDrop 2000 spectrophotometer	Thermo Scientific	https://www.thermofisher.com/us/en/home.html

RESOURCE AVAILABILITY

Lead contact

Further information and requests for resources and reagents should be directed to and will be fulfilled by the lead contact, Takayuki Kohchi (tkohchi@lif.kyoto-u.ac.jp).

Materials availability

Plasmids and transgenic lines generated during this study are available from the Lead Contact without restriction.

Data and code availability

Data have been deposited at DDBJ/ENA/GenBank databases and are publicly available as of the date of publications. Accession numbers are listed in the Key resources table. This paper does not report original code. Any additional information required to reanalyze the data reported in this paper is available from the lead contact upon request.

EXPERIMENTAL MODEL AND SUBJECT DETAILS

Plant materials and culture

The female accession, Takaragaike-2 (Tak-2), and the male accession, Takaragaike-1 (Tak-1), and their backcrossed female line BC3-38 of *Marchantia polymorpha* ssp. *ruderalis*[19,69,70] were used in this study. The UV plant (Figure 1C) was isolated among progeny sporelings derived from a cross between BC3-38 and Tak-1. These plants were grown primarily on half-strength Gamborg's B5 medium[46] containing 1% agar, or on vermiculite supplemented by 2,000-fold-diluted HYPONeX (Hyponex Japan, Osaka, Japan) under continuous white light (50-60 μmol photons m^{-2} s^{-1}; CCFL OPT-40C-N-L, Optorom) at 22°C. To induce reproductive growth, 10-day-old gemmalings or older thalli were transferred to white light conditions supplemented with far-red light (30 μmol photons m^{-2} s^{-1}, VBL-TFL600-IR730*, Valore, Kyoto, Japan).[69,71]

METHOD DETAILS

Plant transformation

Agrobacterium-mediated transformation of *M. polymorpha* was performed using standard protocols for sporelings[72] for the initial screening or thalli[73] for all the other lines. Transformants were selected on the media containing 100 μg ml^{-1} cefotaxime and either 10 μg ml^{-1} hygromycin or 0.5 μM chlorsulfuron according to the selection marker genes in the binary vectors. After co-cultivation with *Agrobacterium*, plants were washed with sterile water and plated on the selective media. Regenerating antibiotic-resistant transformants (T1) were transferred to new selective media and grown until gemmae (G1) were produced.

U chromosome assembly

Draft genome assembly was performed from PacBio reads using Redbean ver. 2.5[61] with default settings. The draft contigs were polished by NextPolish ver v1.3.1[62] using PacBio long reads and Illumina short reads, followed by a further round of polishing by Pilon ver. 1.23[63] with Illumina short reads. Separately, a draft genome was also reconstructed using NextDenovo v2.2-beta.0 (https://github.com/Nextomics/NextDenovo), NextPolish, and Pilon, which was then merged into the draft genome obtained from Redbean to compensate missing regions based on comparisons with the reference genomes obtained from MarpolBase (MpTak1v5.1 and JGI3.1, https://marchantia.info). The resultant genome sequences were subjected to Hi-C scaffolding with the 3D-DNA pipeline.[64] The *in situ* Hi-C library preparation of 2-week-old Tak-2 thalli, sequencing, and data processing were performed as described previously.[20] Finally, the order and orientation of the contigs within scaffolds were manually corrected by comparing them to the v3.1 genome sex-chromosomes.[19] Gene annotation was lifted-over from the reference genomes by aligning transcript sequences using GMAP ver. 2019.09.12 s.[65] Full-length transcriptome sequences (Iso-seq) and RNA-seq reads were obtained from INSDC (BioProject IDs: PRJDB8530 and PRJNA251267), mapped to the newly obtained Tak-2 genome, and used as evidence for gene annotations. All U chromosome-linked genes were manually curated and spurious gene models that did not show any expression level or share homology to known functional domains were eliminated. New gene models were also identified based on evidence from Iso-seq and RNA-seq. The updated gene IDs for the sex chromosome-linked genes are listed in Data S1A.

Genetic nomenclature

BPCU and BPCV correspond to the locus codes, MpUg00370 (this study) and MpVg00350,[20] respectively. Genetic nomenclature in *M. polymorpha* is as outlined previously.[74] Prefix "Mp" in gene symbols was omitted for simplicity since all genes used in this study were derived from *M. polymorpha*. The gene symbols, *BPCU* and *BPCV*, were renamed from *BPC1* and *BPC2*, respectively, from the reported genome analysis[19] to clearly designate their location on specific sex chromosomes. Locus codes and gene symbols are also available through MarpolBase (https://marchantia.info/).

Microscopy

The stalk of the developing sex organs (archegoniophores or antheridiophores) was cut off, placed on agar medium, and the entire receptacles were photographed with a stereomicroscope SZX16 (OLYMPUS, Tokyo, Japan). The inner gamete-containing organs were removed using a needle on a glass slide and photographed with a microscope Axiophot (ZEISS, Oberkochen, Germany).

RNA extraction and reverse-transcription

Total RNA was extracted from stages 1-2 sex organs[49] or 10-day-old thalli with TRIzol reagent (Thermo Fisher Scientific) according to the manufacture's instruction. DNA in the solution was digested using RQ1 RNase-Free DNase (Promega, Madison, USA) by incubation at 37°C for 15 min. The quantity and quality of extracted RNA were assessed using a NanoDrop 2000 spectrophotometer (Thermo Scientific). 500 ng of total RNA was reverse-transcribed to synthesize the first-strand cDNA using ReverTra Ace (Toyobo Life Science) with a 20-mer oligo dT primer. The synthesized cDNA was diluted 10 times with H_2O and used for the experiments.

Plasmid construction for expressing BPCU and BPCV

Plasmids used in this study were constructed using Gateway cloning system (Thermo Fisher Scientific, Waltham, MA) for *M. polymorpha*,[51,52] as described below. Primers used for PCR amplification are listed in Table S1. The constructs were verified by Sanger sequencing.

To create the vectors for expressing *BPCU* and *BPCV* in plants, the gene sequences of *BPCU* (2-kb upstream to 3-kb downstream of the transcribed region) and *BPCV* (1.5-kb upstream to 2-kb downstream of the transcribed region) were amplified from Tak-2 and Tak-1 genomic DNAs, respectively, using KOD FX Neo DNA polymerase (Toyobo Life Science, Osaka, Japan), and cloned into pENTR/D-TOPO (Thermo Fisher Scientific). The resulting entry vectors (BPCU-gene-pENTRdTOPO and BPCV-gene-pENTRdTOPO) were recombined with pMpGWB101[51] and pMpGWB301[51] using Gateway LR clonase II Enzyme mix (Thermo Fisher Scientific) to create BPCU-gene-pMpGWB101, BPCU-gene-pMpGWB301, and BPCV-gene-pMpGWB301.

To create the vectors for the expression of *BPCU* and *BPCV* proteins in *Escherichia coli*, the coding sequences (CDSs) of *BPCU* and *BPCV* were amplified by RT-PCR from Tak-2 and Tak-1 thallus RNA using KOD FX Neo DNA polymerase and KOD One PCR Master Mix (Toyobo Life Science), respectively. These PCR products were cloned into pENTR D-TOPO (Thermo Fisher Scientific) to generate BPCU-cds-pENTRdTOPO and BPCV-cds-pENTRdTOPO. These entry vectors were recombined with pET-DEST42 using Gateway LR clonase II Enzyme mix to create BPCU-cds-pET-DEST42 and BPCV-cds-pET-DEST42. These vectors were introduced into *E. coli* BL21-RIL cells for the protein expression described below.

Genome editing

To generate mutants for *BPCU* (*bpcU-101*, *bpcU-102*, and *bpcU-3*), *BPCV* (*bpcV-1, bpcV-2* and *bpcV-3*) and *FGMYB* (*fgmyb-31* and *fgmyb-41*), oligonucleotides listed in Table S1 were used as guide RNA (gRNA) sequences for CRISPR/Cas9-mediated genome editing with pMpGE_En03 (Addgene 71353), and pMpGE010 (Addgene 71536) or pMpGE011 (Addgene 71537).[52] To generate large deletion mutants for *BPCU* (*bpcU-1* and *bpcU-2*), four pairs of oligonucleotides (Table S1) were cloned as gRNA sequences into pMpGE_En04, pBC-GE12, pBC-GE23, and pBC-GE34,[53] and further combined to generate an entry clone having four gRNAs. The resultant gRNA sequences were subcloned into pMpGE017 by the Gateway LR reaction as described previously.[53] For the initial Feminizer screening, the gene-edited mutants were generated via transformation of F1 spores from a cross between Tak-2 and Tak-1 with the above constructs. *bpcU* mutants (*bpcU-1* and *bpcU-2*) and *bpcV* mutants (*bpcV-1, bpcV-2,* and *bpcV-3*) were generated in Tak-2 and Tak-1, respectively, and *bpcU-3* in the BC3-38 background, via thallus transformation.

Genotyping and sex diagnosis

Genomic DNA was extracted from a small piece of thallus (3 mm x 3 mm) crushed with micropestle in 100 μL of genotyping buffer containing 100 mM Tris-HCl, pH 9.5, 1M KCl, and 100 mM EDTA as described previously,[75] and used for PCR using KOD FX Neo DNA polymerase. For gene-edited mutant identification, gRNA-targeted regions were amplified from the genomic DNA of transformants, and sequenced using the primer pairs listed in Table S1. Sex diagnosis was performed using the primer sets for *rhf73* and *rbm27* that are specific to sex chromosomes as described previously.[76]

Generation of transgenic lines expressing genomic BPCU and genomic BPCV

To create the transgenic plants carrying the *BPCU* and *BPCV* transgenes, thallus transformation[73] was used to introduce BPCU gene pMpGWB101 and BPCU gene pMpGWB301 into Tak-1 and *bpcU-1*, respectively, and also BPCV gene pMpGWB301 into *bpcU-1*. To confirm genomic integration of the transgenes, G1 gemmae were used for PCR amplification using KOD One PCR Master Mix and primers listed in Table S1, and progeny of G1 plants were used for the experiments. More than 10 lines were independently isolated for each construct, and the data from multiple representative lines were shown.

RT-PCR

RT-PCR was performed in 10 μL reaction solution, containing KOD One PCR Master Mix, 1 μL diluted cDNA and 0.3 μL each of 10 μM forward and reverse primers listed in Table S1 *PRM* (Mp3g14390) and *LC7* (Mp6g01560) were amplified under the following cycle conditions: initial incubation at 94°C for 2 min, followed by 37 cycles of 98°C for 10 s, 58°C for 5 s and then 68°C for 1 s. Mp5g13880 was amplified under the following cycle conditions: initial incubation at 94°C for 2 min, followed by 35 cycles of 98°C

for 10 s, 60°C for 5 s and then 68°C for 1 s. Mp7g02820 was amplified under the following cycle conditions: initial incubation at 94°C for 2 min, followed by 35 cycles of 98°C for 10 s, 58°C for 5 s and then 68°C for 1 s. *EF1* (Mp3g23400) was amplified under the following cycle conditions: initial incubation at 94°C for 2 min, followed by 31 cycles of 98°C for 10 s, 58°C for 5 s and then 68°C for 1 s.

Quantitative real-time RT-PCR

Quantitative real-time RT-PCR (qRT-PCR) was performed in 25 μL reaction solution, containing homemade Taq DNA polymerase,[47] SYBR Green I Nucleic Acid Gel Stain (Lonza, Basel, Switzerland), 5 μL diluted cDNA, and 1 μL each of 10 μM forward and reverse primers listed in Table S1. Reactions were carried out with a CFX96 real-time PCR detection system (Bio-Rad Laboratories, Hercules, CA), under the following cycle conditions: initial incubation at 95°C for 30 s, followed by 40 cycles of 95°C for 5 s, and 60°C for 30 s. Three technical and three biological replicates were measured for each reaction. *EF1* (Mp3g23400) was used as internal control.[77] Relative expression levels were calculated by the $2^{-\Delta\Delta CT}$ method.[78]

DPI-ELISA with BPCU and selected DNA-probes

E. coli BL21-RIL cells harboring BPCU-cds-pET-DEST42 or BPCV-cds-pET-DEST42 were used for the protein expression. Crude protein extraction was performed with HEPES buffer (4 mM HEPES pH 7.5, 100 mM KCl, 8% (v/v) glycerol, 0.2% biotin-free BSA, 5 mM dithiothreithol (DTT), supplemented with 1x cOmplete Protease Inhibitor without EDTA (Roche, Basel, Switzerland).[79] Protein extracts from non-transformed *E. coli* BL21-RIL cells served as controls. Semiquantitative DPI-ELISA experiments were performed with 5 μg of crude protein extracts (in 30 μl buffered solution) and biotinylated double-stranded (ds) DNA-probes.[80] Promoter probes were PCR amplified by using biotinylated (sense) and non-biotinylated (antisense) primer combinations. Residual biotinylated primers were removed with a NucleoSpin Gel and PCR Clean-up Kit (Macherey & Nagel, Duren, Germany). DPI-ELISA with purified promoter probes was performed according to the general protocol.[79] The use of streptavidin-coated ELISA plates (5 pmol/well) allows for the semiquantitative and comparable readout within the same protein extract.[32,80] Pre-blocked clear flat-bottom Streptavidin Coated Plates (96-wells) (Pierce Thermo Fischer Scientific) were used with Safire II multiplate reader (Tecan, Mannedorf, Switzerland) for photometric measurements. Detection of 6xHis-epitope tagged BPCU was carried out with either Penta·His HRP Conjugate Kit (QIAGEN, Hilden, Germany) or HRP Anti-6X His tag antibody (Abcam, Cambridge, UK) and ortho-phenylenediamine (OPD) as a substrate. The HRP reaction was stopped in all wells by addition of sulfuric acid (2 N H_2SO_4) as soon as a visible coloration appeared. Average signal intensities and standard deviation were computed from two technical replicates on the same plate and from two independent protein extracts. Relative signal intensities were calculated relative to the highest photometric absorbance of a reference protein-DNA combination.

Flow cytometry analysis

Flow cytometry was performed according as previously described[81] with slight modifications. One hundred mg of 9-day-old *M. polymorpha* thalli and 37-day-old *A. thaliana* (Col-0) rosette leaves were chopped in 1.5 mL of Galbraith Buffer (45 mM $MgCl_2$, 30 mM Trisodium citrate dihydrate, 20 mM MOPS, pH 7.0) supplemented with 0.1% v/v Triton X-100 using a single edge blade (AccuTec Blades, Verona, USA) for 5 min on ice, and consecutively passed through 40 μm (Corning, NY, USA), 20 μm and 10 μm cell strainers (SYSMEX, Kobe, Japan). RNaseA (Sigma-Aldrich, St. Louis, USA) was added to a final concentration of 50 μg ml^{-1} and incubated on ice for 15 min, then propidium iodide (Nacalai Tesque, Kyoto, Japan) was added to the same final concentration and incubated on ice for 30 min. The prepared samples were analyzed by a BD Accuri C6 Flow Cytometer (BD Biosciences, Franklin Lakes, USA) for 300,000 events each.

Chromatin profiling analysis

The CUT&RUN (Cleavage Under Targets & Release Using Nuclease) assays were performed as previously described[48] with slight modifications.[20] DAPI stained 40,000 nuclei were sorted by BD FACSARIA III (BD Biosciences). 10 μL of BioMagPlus Concanavalin A bead slurry (Polysciences, #86057) was washed twice in 700 μL of binding buffer (20 mM HEPES pH 7.9, 10 mM KCl, 1 mM $CaCl_2$ and 1 mM $MnCl_2$) and resuspended in 10 μl of binding buffer, and added to the nuclear suspension. The mixture was thoroughly mixed on a rotator for 10 min at room temperature to allow binding of nuclei to the beads. The nuclei were pelleted with a magnet stand and resuspended with 50 μl of antibody buffer (20 mM HEPES pH 7.5, 150 mM NaCl, 0.5 mM spermidine, 1 × protease inhibitor cocktail EDTA free (Roche) and 2 mM EDTA pH8.0). 0.5 μg of antibody was thoroughly mixed and incubated overnight at 4°C. Nuclei were washed twice on a magnet stand with 1 mL of wash buffer and incubated with 700 ng μl^{-1} of Protein A–micrococcal nuclease fusion protein (pA-MN) in 50 μl of wash buffer at room temperature. After 10 minutes, the mixture was washed twice with 1 mL wash buffer to remove unbound pA-MN. Nuclei were resuspended in 150 μl of wash buffer and chilled on ice at 0°C. 3 μl of 100 mM $CaCl_2$ was added to activate pA-MN with incubation at 0°C for 120 min. The reaction was stopped by the addition of 100 μl of 2 × STOP buffer (340 mM NaCl, 20 mM EDTA, 4 mM EGTA, 50 μg ml^{-1} RNase A, 50 μg ml^{-1} glycogen and MNase digested spike-in DNA (HEK293 cells)) and incubated in thermo-mixier at 37°C for 10 minutes at 500 rpm. The protein–DNA complex was released by centrifugation and then digested by 0.05 mg proteinase K and 0.1% SDS at 70 °C for 10 min. DNA was extracted by Phenol: Chloroform: Isoamyl-alcohol (25:24:1) with phase lock gel tubes. Library preparation of CUT&RUN was performed using a NEB Ultra II library preparation kit. 150-500 bp of DNA was selected by SPRI beads. DNA amount and fragment size were analyzed

by Nanodrop 3300 and Fragment analyzer respectively. Libraries were pooled at similar molar amounts and sequenced using the Nextseq 500 platform. Paired-end sequencing was performed (read length, 42 bp × 2; index, 6 bp).

Analysis of sex chromosome evolution

Predicted orthologs of *M. polymorpha* gametolog were collected from available liverwort genome and transcriptome sequence data.[82–86] Since the available liverwort transcriptomes were not generated to investigate sex chromosome evolution, we initially applied two filters. First, sequences derived from monooicous species were removed as monoicy is associated with a loss of sex chromosomes. Second, for analyses of gametologs other than BPC, we included only dioicous liverwort species for which only a single sex appeared to be sampled, because the transcriptome data appeared to be derived from a single sex (based on the presence of a single gametolog for each gene that we inferred to be in the oldest evolutionary stratum). An exception was the Haplomitriopsida species, where we included all identified sequences since these sequences were critical for identifying the oldest evolutionary stratum. For the phylogenetic analysis of BPC orthologs, all identified sequences from dioicous liverwort species were included. Moss and hornwort orthologs were also included to ascertain whether any non-recombining regions pre-date the origin of liverworts, and vascular plant (lycophyte and fern) orthologs were used to root the trees.[83,86]

For phylogenetic analyses of the gametologs (Figure 4; Data S2), all site types in coding regions (including non-synonymous as well as synonymous sites) were used. Complete or partial coding nucleotide sequences were manually aligned as amino acid translations using Se-Al v2.0a11 for Macintosh (http://tree.bio.ed.ac.uk/software/seal/). Poorly alignable sequences were removed, and alignments of nucleotides were employed in subsequent Bayesian analysis using MrBayes 3.2.1.[66,67] The analysis was run for 1,000,000 generations (except for *BPCU*/MpUg00370 which was run for 10,000,000 generations), which was sufficient for convergence of the two simultaneous runs (split frequencies < 0.05). To allow a burn-in phase, the first 50% of the trees generated were discarded. The graphic representation of the trees was generated using the FigTree (version 1.4.0) software (http://tree.bio.ed.ac.uk/software/figtree/). Sequence alignments and command files used to run the Bayesian phylogenetic analyses can be provided upon request.

The proportions of synonymous substitutions per synonymous site (Ks values) were calculated with SNAP v2.1.1 (https://hcv.lanl.gov/content/sequence/SNAP/SNAP.html) as described previously.[68,87] Ks values for the 19 pairs of *M. polymorpha* gametologs were previously reported.[19] To relate these values to the liverwort phylogeny, we aligned sequences of eleven autosomal orthologs of liverwort genes across the same phylogenetic groups as used for studying gametologs, and estimated Ks values separately for each gene, with the standard deviation calculated as a measure of variation in values of different genes at each phylogenetic node (Data S1B).

Data analysis of CUT&RUN

CUT&RUN reads were preprocessed to filter out low-quality reads with Fastp v0.20.1,[54] and mapped to the MpTakv6 genome presented in this paper using Bowtie2 v2.4.1[56] with the "–very –sensitive" flag. Reads with MapQ less than 10 were removed with Samtools v1.9.0,[58] and duplicates or inserts less than 140 bp reads were removed with alignmentSieve in Deeptools v3.5.0.[59] Deduplicated reads from biological replicates were merged. We called peaks for chromatin marks by SICER2 with default parameters.[30] Bigwig files were generated using "bamcoverage" in Deeptools[59] with "–extendReads –exactScaling –binSize 10 –normalizeUsing RPGC" flags. The effective genome size was calculated from MpTakv6 with faCount.

Transcriptome Mapping

RNA-seq reads were preprocessed to filter out low-quality reads with Fastp v0.20.1,[54] and mapped to the MpTakv6 genome presented in this paper using STAR v2.7.3a[57] with default parameters. Bigwig files were generated using "bamcoverage" in Deeptools[59] with "–binSize 10 –normalizeUsing BPM" flags.

QUANTIFICATION AND STATISTICAL ANALYSIS

General statistical analyses

All statistical analyses were conducted in R (version 3.6.0). The specific tests, sample, size, and p value are displayed in the corresponding legends.

Gene expression analysis of BPCU and BPCV

Gene expression data from female sex organs: DRR050351, DRR050352, DRR050353,[49] male sex organs: DRR050346, DRR050347, DRR050348,[49] female thalli: DRR118943, DRR118944, DRR118945,[50] male thalli: DRR118949, DRR118950, DRR118951,[50] spores: SRR4450260, SRR4450261, SRR4450262,[19] and sporelings: SRR4450254, SRR4450255, SRR4450256[19] were downloaded from Sequence Read Archive. Transcript abundances were quantified by Salmon package v1.40 with–validateMappings option.[55] Transcripts Per Million values of transcripts were integrated into values corresponding to genome annotations by tximport package.[60]